Body temperature drives azole tolerance in *Candida albicans* by hindering the autophagic degradation of Erg11

Yanru Feng[1], Cheng Zhen[1], Wanqian Li[1], Malcolm Whiteway[2], Xinyu Fang[1], Xuqing Shen[1], Hui Lu[1*], Yuanying Jiang[1*]

1. Department of Pharmacy, Shanghai Tenth People's Hospital, School of Medicine, Tongji University, Shanghai, China.
2. Department of Biology, Concordia University, Montreal, QC, Canada

***To whom correspondence should be addressed:**

Hui Lu

Associate Senior Research Fellow in the Department of Pharmacology, Shanghai Tenth People's Hospital, School of Medicine, Tongji University

No.1239 Siping Road, Shanghai, 200092, China.

E-mail: luhui2019@tongji.edu.cn (HL)

Yuanying Jiang

Professor in the Department of Pharmacology, Shanghai Tenth People's Hospital, School of Medicine, Tongji University

No.1239 Siping Road, Shanghai, 200092, China.

E-mail: jiangyy@tongji.edu.cn (YYJ)

Abstract

Human body temperature has been shown to limit the antifungal efficacy of azoles; however, the precise mechanisms underlying this limitation remain insufficiently understood. In this study, we observed that brief exposure (24 h) to human body temperature (37 °C), in contrast to 30 °C, significantly enhances the tolerance of *Candida albicans* to azoles without inducing resistance. Our findings suggest that this increased tolerance is due to a reduction in the degradation of *C. albicans* Erg11 at 37 °C compared to 30 °C, thereby promoting azole tolerance. This phenomenon occurs because Erg11 degradation is mediated by autophagy, which is inhibited in *C. albicans* at 37 °C. The suppression of autophagy at this temperature may be associated with elevated mitochondrial production of reactive oxygen species, leading to mitochondrial dysfunction. In response to heat stress-induced mitochondrial dysfunction, autophagy-related proteins such as Atg8 accumulate around the mitochondria, while their levels in the endoplasmic reticulum decrease, consequently inhibiting autophagy in *C. albicans*. These findings suggest that promoting the degradation of Erg11 in *C. albicans* may serve as a viable strategy to augment the fungicidal efficacy of azoles in the human host.

Keywords: Erg11 degradation, azole tolerance, autophagy, heat stress, *Candida albicans*.

41 **Introduction**

42 In recent years, the morbidity and mortality rates associated with candidiasis have
43 remained consistently high, presenting significant threats to public health and imposing
44 a substantial medical burden[1]. Recent epidemiological data suggest that approximately
45 1.56 million individuals are affected by candidiasis annually, resulting in approximately
46 100,000 fatalities[2]. Azoles have emerged as the most frequently utilized antifungal
47 agents for the clinical prevention and treatment of fungal infections, owing to their
48 broad antimicrobial spectrum, favorable safety profile, and diverse routes of
49 administration[3]. However, a primary challenge associated with azole therapy is their
50 fungistatic nature, which allows *Candida albicans* to develop tolerance to azoles,
51 ultimately leading to resistance[4]. The azole tolerance exhibited by *C. albicans* is
52 evidenced by its ability to proliferate at azole concentrations surpassing the minimum
53 inhibitory concentration (MIC). Although the prevalence of fluconazole (FLC)
54 resistance in *C. albicans* is generally low, reported at less than 1%[5], FLC often proves
55 ineffective in treating candidiasis caused by susceptible *C. albicans* isolates. The
56 observed discrepancy between overall treatment outcomes and minimal levels of
57 clinical resistance is likely attributable to multiple factors[6]. Nevertheless, FLC tolerance
58 in *C. albicans* is a critical consideration, as both in vitro and in vivo antifungal efficacy
59 of FLC is substantially reduced against *C. albicans* strains exhibiting high azole
60 tolerance[7]. Furthermore, elevated levels of FLC tolerance are associated with persistent
61 candidemia[8,9], which contributes to approximately 50% of the mortality associated with
62 neonatal candidiasis[10]. However, the specific factors and mechanisms regulating the
63 tolerance of *C. albicans* to azoles within the human host environment remain unclear.

64 It has been reported that the human body temperatures play a critical role in driving the
65 development of drug resistance in pathogenic fungi. Studies have shown that, compared
66 to a culture temperature of 30 °C, a temperature of 37 °C can decrease the susceptibility
67 of *C. albicans* to azoles[11,12]. Research on the fungal pathogen *Rhodosporidiobolus*
68 *fluvialis* suggests that exposure to mammalian body temperature can induce
69 mutagenesis, leading to the emergence of hypervirulent and pan-drug-resistant strains[13].
70 Moreover, it has been demonstrated that anthropogenic global warming significantly

affects azole resistance[14,15], with increased occurrences of azole-resistant *Aspergillus fumigatus* and *Candida parapsilosis* reported in warmer environments, such as greenhouses[16] and tropical regions[17,18]. Additionally, the rapid global spread of multidrug-resistant *Candida auris* in humans has been linked to temperature adaptation driven by climate warming[19,20]. Body temperature may influence fungal drug susceptibility through non-genetic mechanisms within the human host[21]. However, the exact mechanisms by which short-term exposure to body temperature reduces fungal susceptibility to azoles have yet to be elucidated. This gap in understanding poses a challenge for developing targeted antifungal strategies aimed at enhancing the efficacy of azoles in human hosts.

In this study, we observed that a short-term exposure (24 h) to the human body temperature of 37 °C increases azole tolerance, but not azole resistance, in *C. albicans.* Our investigations further revealed that Erg11 is subject to degradation via the autophagy pathway. However, exposure to a body temperature of 37 °C, as opposed to 30 °C, inhibits autophagy, thereby decelerating the degradation rate of Erg11. This process ultimately enhances the tolerance of *C. albicans* to azoles. These findings expand the conceptual framework of azole tolerance mechanisms in *C. albicans*, demonstrating that the human host body temperature can modulate the degradation rate of the azole drug target Erg11 through epigenetic regulatory pathways.

Results

Short-term exposure to body temperature enhances the tolerance of *C. albicans* to azoles

At a physiological body temperature of 37 °C, compared to 30 °C, we observed a decrease in the susceptibility of the *C. albicans* wild-type strain SN152 to FLC (Figure 1a). However, it remains uncertain whether this decreased drug susceptibility is due to an increase in the resistance level or tolerance level of *C. albicans* to FLC. In this study, we characterized the enhancement of FLC resistance in *C. albicans* by assessing the elevation of the minimum inhibitory concentration (MIC) value of FLC, while the increase in the super-MIC growth (SMG) value was used to represent the elevation of FLC tolerance in *C. albicans*[8,22](Figure 1b). Our findings indicate that, compared to

101 30 °C, the temperature of 37 °C significantly increased the SMG value of FLC against
102 the strain SN152 from 0.070 to 0.440, whereas the MIC value of FLC against the strain
103 SN152 remained constant at 0.5 μg/ml (Figure 1c). Cyclosporin A, a known calcineurin
104 inhibitor, was observed to abolish the tolerance of *C. albicans* to FLC by reducing the
105 SMG value of FLC, but not affect the resistance of *C. albicans* to FLC, as indicated by
106 the unchanged MIC value[8,22]. Our study demonstrated that the decreased susceptibility
107 of *C. albicans* to FLC after incubation at 37 °C for 24 h was reversed by cyclosporin A
108 (Extended Data Figure 1a). Furthermore, the deletion of the *CDR1* gene, which encodes
109 the efflux pump Cdr1, resulted in a reduced MIC value of FLC against *C. albicans*, yet
110 it did not eliminate FLC tolerance in the organism[8,23]. Our findings indicated that, in
111 comparison to 30 °C, culturing at 37 °C further diminished the susceptibility of the *C.*
112 *albicans cdr1*Δ/Δ null mutant to FLC (Extended Data Figure 1b). This observation is
113 attributed to the physiological temperature, which increased the SMG value of FLC
114 against the *cdr1*Δ/Δ null mutant, although it did not elevate the MIC value for this
115 mutant (Figure 1c). These results suggest that the reduced susceptibility of *C. albicans*
116 to FLC following short-term exposure (24 h) to physiological temperature is primarily
117 due to an enhanced tolerance, rather than the development of resistance of *C. albicans*
118 to azoles.
119 Our investigation revealed that elevating the culture temperature from 30 °C to 37 °C
120 significantly increased the SMG values of FLC against clinical isolates of *C. albicans*
121 (n = 104), *Candida glabrata* (n = 10), *Candida parapsilosis* (n = 10), *Candida krusei*
122 (n = 10), and *Candida guilliermondii* (n = 10) (Figure 1d). This observation suggests
123 that physiological body temperature generally enhances the tolerance of *Candida*
124 species isolates to FLC. Additionally, the SMG values for itraconazole, miconazole,
125 ketoconazole and voriconazole against *C. albicans* were significantly elevated when
126 cells were cultured at 37 °C (Figure 1e). Moreover, the antifungal efficacy of other
127 ergosterol biosynthesis inhibitors, such as terbinafine (targeting Erg1) and fluvastatin
128 (targeting Hmg1), were reduced at 37 °C (Figure 1f). However, the culture temperature
129 did not affect the antifungal activity of amphotericin B (binding and destroying plasma
130 ergosterol), caspofungin (targeting Fks1 to inhibit the synthesis of 1,3-β-D-glucan),

131 tunicamycin (inducing ER stress), myriocin (blocking serine-palmitoyltransferase in
132 sphingolipid biosynthesis) and staurosporine (inhibiting protein kinase C) against *C.*
133 *albican*s (Extended Data Figure 1c). Overall, these findings indicate that brief exposure
134 to physiological body temperature substantially increases the tolerance of *C. albicans*
135 to azoles.

136 **The augmented tolerance of *C. albicans* to azoles at body temperature is dependent**
137 **on Erg11**

138 Upon brief exposure to body temperature, *C. albicans* exhibited reduced susceptibility
139 to inhibitors targeting ergosterol biosynthesis, including azoles, terbinafine and
140 fluvastatin (Figures 1e and 1f). Conversely, this exposure did not significantly impact
141 the efficacy of inhibitors targeting non-ergosterol biosynthesis pathways, such as
142 caspofungin, tunicamycin, myriocin, and staurosporine (Extended Data Figure 1c).
143 Furthermore, our study demonstrated that both fluvastatin (1 μg/ml) and terbinafine (1
144 μg/ml) effectively decreased the SMG values of FLC against *C. albicans* at 37 °C
145 (Figure 2a). These findings suggest that exposure to body temperature may influence
146 the ergosterol biosynthesis pathway in *C. albicans*, thereby enhancing its tolerance to
147 azoles.

148 We proceeded to delete the *EFG1*, *NDT80*, and *UPC2* genes in *C. albicans*, which
149 encode transcriptional regulators involved in ergosterol biosynthesis[24-27]. Our findings
150 demonstrated that at 37 °C, there was an increase in the SMG value of FLC against the
151 *efg1*Δ/Δ and *ndt80*Δ/Δ null mutants (Extended Data Figure 2a). In contrast, the
152 *upc2*Δ/Δ null mutant consistently exhibited low MIC and SMG values for FLC at both
153 30 °C and 37 °C (Figure 2b). This observation was further corroborated by spot assays,
154 which confirmed that 37 °C did not reduce the susceptibility of the *upc2*Δ/Δ null mutant
155 to FLC (Extended Data Figure 2b). These results suggest that Upc2 may contribute to
156 the tolerance of *C. albicans* to azoles at physiological body temperature.

157 Body temperature may activate Upc2 transcription, thereby enhancing azole tolerance
158 in *C. albicans*. We tagged the C-terminal of Upc2 with GFP, and subsequent laser
159 confocal microscopy demonstrated that brief exposure to body temperature did not
160 influence the nuclear import of Upc2 in *C. albicans* in the presence of FLC (16 μg/ml)

161 (Extended Data Figures 2c and 2d). Furthermore, RNA-seq analysis indicated that
162 short-term exposure to 37 ℃ (for 4 h, 8 h, and 16 h) did not significantly alter the
163 transcription levels of most ergosterol synthesis genes (Extended Data Figure 2e).
164 Additionally, we tagged the C-terminal regions of key enzymes involved in ergosterol
165 biosynthesis with GFP, including Erg6, Erg9, Erg10, Erg11, Erg12, Erg13, Erg20,
166 Erg26, and Erg251. Consistent with the RNA-seq findings, no upregulation of these
167 enzymes was observed at 37 °C compared to 30 °C. In fact, western blot analysis
168 suggested a slight decrease in expression levels at 37 °C (Figures 2c and 2d).
169 Furthermore, the analysis conducted using gas chromatography-mass spectrometry
170 (GC-MS) indicated that there were no notable differences in intracellular ergosterol
171 concentrations between the two temperature conditions at the 4-hour, 8-hour, and 16-
172 hour incubation intervals (Extended Data Figure 2f). These results collectively imply
173 that the enhanced tolerance of *C. albicans* to azoles at 37 °C is not mediated by the
174 activation of Upc2 transcriptional activity.
175 In *C. albicans*, Erg7 (lanosterol synthase) catalyzes the conversion of squalene epoxide
176 to lanosterol. This lanosterol is subsequently transformed into eburicol through the
177 activity of Erg6 (Δ-(24)-sterol C-methyltransferase). Following this conversion, Erg11
178 mediates the oxidative demethylation of the 14-α-methyl group from eburicol,
179 producing 4,4-dimethylcholesta-8,14,24-trienol[28]. Inhibition of Erg11 by azoles
180 induces an alternative biosynthetic pathway involving Erg251 (C-4 sterol methyl
181 oxidase), Erg26 (C-3 sterol dehydrogenase), Erg27 (3-keto sterol reductase), and Erg3
182 (C-5 sterol desaturase), which results in the synthesis of compensatory sterols that retain
183 14α-methyl groups[22] (Figure 2e). GC-MS analysis demonstrated a significant reduction
184 in lanosterol levels, with no statistically significant changes in obtusifoliol
185 concentrations, when cells were exposed to 16 μg/ml FLC at 37 °C compared to 30 °C
186 (Figure 2f). Furthermore, utilizing the *ADH1* promoter to enhance the expression of
187 ergosterol biosynthesis genes in the *upc2*Δ/Δ null mutant, specifically *ERG2*, *ERG4*,
188 *ERG6, ERG9*, *ERG11*, *ERG24, ERG26*, and *ERG27*, showed that only the upregulation
189 of *ERG11* significantly improved the relative growth of *C. albicans* under FLC
190 exposure (0.25 μg/ml) at 37 °C (Figure 2g). These results are corroborated by chemical

191 genomics experiments, which demonstrated that fluvastatin, targeting Hmg1, and
192 terbinafine, targeting Erg1 — both acting upstream of Erg11 — can inhibit azole
193 tolerance induced by heat stress (Figure 2a). Conversely, amorolfine, which targets
194 Erg24 and is positioned downstream of Erg11[29], did not show a similar inhibitory effect
195 (Extended Data Figure 2g). Additionally, a notable increase in FLC tolerance was
196 observed in the *erg24*Δ/Δ null mutant at 37 °C (Extended Data Figure 2h). The deletion
197 of either the *ERG251* or *ERG3* gene[22], which are components of an alternative pathway,
198 did not abolish the heat stress-induced tolerance to azoles (Extended Data Figure 2i).
199 These findings suggest that body temperature augments the tolerance of *C. albicans* to
200 azoles via a mechanism reliant on Erg11.

201 **Body temperature inhibits the degradation of Erg11**

202 We further modulated the expression of the *ERG11* and *ENO1* genes in the
203 *ERG11*/*erg11*Δ and *ENO1*/*eno1*Δ heterozygous deletion mutants using the doxycycline
204 (DOX)-inducible Tet-off promoter system (Extended Data Figure 3a). This system
205 facilitates the regulation of the transcription levels of the *ERG11* and *ENO1* genes in
206 response to varying DOX concentrations (Extended Data Figure 3b). Notably, the MIC
207 values of DOX against the $P_{tet\text{-}off}$-*ENO1*/*eno1*Δ mutant remained consistent at both
208 30 °C and 37 °C. Conversely, the MIC value of DOX against the $P_{tet\text{-}off}$-*ERG11*/*erg11*Δ
209 mutant at 37 °C was observed to be twice as high as at 30 °C (Figure 3a). These findings
210 indicate that the increased tolerance of *C. albicans* to FLC at 37 °C cannot be attributed
211 to the expression level of Erg11 at this temperature.

212 Moreover, the induction of azole tolerance by body temperature was determined to be
213 contingent upon the culture medium. Specifically, an increased azole tolerance
214 phenotype at 37 °C was observed in the nutrient-rich YPD medium, whereas this was
215 not the case in the nutrient-poor SD medium (Figure 3b). These results imply that the
216 heightened tolerance of *C. albicans* to FLC at 37 °C cannot be ascribed to an augmented
217 catalytic activity of Erg11 at this temperature.

218 Cycloheximide (CHX) chase analysis was employed to assess the degradation rates of
219 Erg11 at 30 °C and 37 °C. The analysis revealed that, unlike at 30 °C, the degradation
220 of Erg11 was markedly inhibited at 37 °C (Figures 3c and 3d). At 37 °C, the inhibition

221 of Erg11 degradation leads to the sustained preservation of its catalytic activity. As a
222 result, *C. albicans* requires a reduced amount of Erg11 to produce an equivalent amount
223 of ergosterol at 37 °C compared to 30 °C. This induces a sterol-mediated negative
224 feedback mechanism that decreases Erg11 levels in *C. albicans* at 37 °C in the absence
225 of FLC (Figures 3e and 3f). However, when FLC inhibits Erg11 activity, the resulting
226 reduction in ergosterol content triggers an upregulation of Erg11 expression. Given that
227 37 °C suppresses Erg11 degradation, the exposure of azoles leads to elevated levels of
228 Erg11 protein in *C. albicans* at 37 °C relative to 30 °C (Figures 3e and 3f), thereby
229 enhancing the azole tolerance of *C. albicans.*

230 **Erg11 undergoes degradation through autophagy**

231 In *S. cerevisiae,* it has been documented that Erg11 is subject to degradation via the
232 Asi-mediated Endoplasmic Reticulum-Associated Degradation (ERAD) pathway
233 following ubiquitination[30-32]. However, the precise mechanism by which ubiquitinated
234 Erg11 is degraded in *C. albicans*—whether through the 26S proteasome or autophagy
235 in *C. albicans*—remains unclear. To investigate the degradation pathway of Erg11 in
236 *C. albicans*, we employed wortmannin, an autophagy inhibitor[33], and MG132, a
237 proteasome inhibitor[34], to ascertain their effects on Erg11 degradation. Our results
238 demonstrated that wortmannin significantly enhanced the FLC tolerance of *C. albicans*
239 at 30 °C and further augmented FLC tolerance at 37 °C. Conversely, MG132
240 diminished FLC resistance at both 30 °C and 37 °C, and reduced FLC tolerance at 37 °C
241 (Figure 4a). Moreover, CHX chase analysis revealed that wortmannin, but not MG132,
242 inhibited the degradation of Erg11 at 30 °C (Figures 4b and 4c). We employed the
243 CellTracker Blue CMAC dye to stain vacuoles and tagged Erg11 with GFP. Laser
244 confocal microscopy experiments revealed that Erg11 was localized within vacuoles,
245 as indicated by the co-localization of green and red fluorescence, resulting in a yellow
246 fluorescence signal (Figures 4d and 4e). Furthermore, our findings revealed that
247 incubation at 37 °C, as opposed to 30 °C, significantly hindered the entry of Erg11 into
248 vacuoles (Figures 4d and 4e). These results collectively suggest that Erg11 undergoes
249 degradation via autophagy, and that this process may be inhibited at 37 °C, thereby
250 suppressing the degradation of Erg11.

251 **Body temperature inhibits autophagy in *C. albicans***

252 Considering that body temperature inhibits the degradation of Erg11, through the
253 autophagy pathway, it can be posited that body temperature may suppress the
254 autophagic process in *C. albicans*. To investigate this hypothesis, we employed a *C.*
255 *albicans* GFP-Atg8 mutant, in which GFP was fused to the N-terminus of Atg8[35].
256 During the activation of autophagy, GFP-Atg8 localizes to autophagosomes and is
257 subsequently released into vacuoles. Notably, GFP exhibits greater resistance to
258 vacuolar hydrolases, leading to the degradation of Atg8 while GFP remains intact. Thus,
259 the conversion of GFP-Atg8 to GFP serves as an indicator of autophagic activity. Our
260 findings indicated that at 37 °C, the ratio of GFP to GFP-Atg8 was significantly lower
261 compared to that observed at 30 °C (Figures 5a and 5b). Additionally, laser confocal
262 microscopy demonstrated that at 30 °C, *C. albicans* cells exhibited a higher number of
263 cells with green fluorescent dots, which are indicative of autophagosomes containing
264 GFP-Atg8; conversely, at 37 °C, the number of such cells was markedly diminished
265 (Figures 5c and 5d). In addition, we utilized MitoTracker Deep Red FM dye for
266 mitochondrial labeling, ER-Tracker Red dye for ER labeling, and GFP for Atg8
267 labeling, employing confocal laser scanning microscopy to examine the effects of
268 elevated environmental temperature on the intracellular localization of Atg8. Our
269 findings indicate that, relative to the condition at 30 °C, the proximity of Atg8 to
270 mitochondria increased at 37 °C (Figures 5e and 5f), whereas its colocalization with the
271 ER diminished (Figures 5g and 5h), consequently resulting in the inhibition of
272 autophagy.

273 **Body temperature-induced mitochondrial oxidative damage that inhibits**
274 **autophagy**

275 Research has demonstrated that heat stress induces mitochondrial dysfunction via
276 oxidative stress mechanisms[36]. In this study, we cultured *C. albicans* at 30 °C and 37 °C
277 for 4 h, followed by RNA sequencing analysis. The results revealed that genes
278 differentially expressed and associated with mitochondrial function were the most
279 enriched, suggesting that exposure to 37 °C may impair mitochondrial function (Figure
280 6a). To further investigate, we employed 2′,7′-dichlorofluorescin diacetate (DCFH-DA)

281 to quantify reactive oxygen species (ROS) levels and observed that the 37 °C condition,
282 compared to 30 °C, resulted in elevated ROS levels in *C. albicans* (Figure 6b).
283 Furthermore, the antioxidant N-acetyl cysteine (NAC) was shown to effectively reduce
284 ROS levels and synergize with FLC to mitigate the tolerance of *C. albicans* at 37 °C
285 (Figure 6c). These findings collectively suggest that mitochondrial oxidative damage
286 in *C. albicans* induced by body temperature may contribute to the increased tolerance
287 of *C. albicans* to azoles.
288 Under conditions of heat stress, Atg8 in plants has been documented to engage
289 biological processes beyond autophagy, including its relocation to the Golgi apparatus
290 to facilitate Golgi reorganization[37]. Consequently, we hypothesized that the
291 redistribution of Atg8 may provide protection to mitochondria against oxidative
292 damage induced by body temperatures. To test this hypothesis, we generated an
293 *atg8*Δ/Δ null mutant in *C. albicans* and assessed the growth rates of both the *atg8*Δ/Δ
294 null mutant and its parental strain SN152 at 30 °C and 37 °C, respectively. Our findings
295 indicated that the *atg8*Δ/Δ null mutant exhibited growth rates comparable to those of
296 the SN152 strain at 30 °C. However, at 37 °C, the *atg8*Δ/Δ null mutant demonstrated
297 reduced growth relative to the SN152 strain (Figure 6d), suggesting that Atg8 plays a
298 critical role in the response to oxidative stress at 37 °C. Additionally, we employed JC-
299 1 to evaluate the impact of the *ATG8* gene on mitochondrial membrane potential
300 (MMP). The lipophilic JC-1 dye, with a delocalized positive charge, accumulates in
301 functional mitochondria, emitting red fluorescence. In dysfunctional mitochondria, it
302 remains dispersed in the cytosol, emitting green fluorescence. A decrease in red and
303 increase in green fluorescence signals mitochondrial dysfunction. Mitochondria with a
304 red-to-green ratio over 1 are considered normal (P1 in Figure 6e), while those below 1
305 are dysfunctional (P2 in Figure 6e). Our findings indicated that at 30 °C, the SN152
306 strain (0.290% ± 0.096%) and the *atg8*Δ/Δ null mutant (0.730% ± 0.131%) exhibit
307 comparable proportions of cells in the P2 region ($P > 0.999$). In contrast, at 37 °C, the
308 *atg8*Δ/Δ null mutant (8.42% ± 0.800%) shows a significantly higher proportion of cells
309 in the P2 region compared to the SN152 strain (5.33% ± 1.19%; $P = 1.07 \times 10^{-2}$)

310 (Figures 6e and 6f). These results suggest that mitochondrial dysfunction in *C. albicans*,
311 triggered by elevated temperatures, may lead to a reduced presence of autophagy-
312 related proteins, such as Atg8, within the ER, thereby inhibiting autophagy.

313 **Discussion**

314 In this study, we observed that short-term exposure of *C. albicans* to the human body
315 temperature of 37 °C, as opposed to 30 °C, results in increased azole tolerance, but not
316 resistance. This phenomenon is primarily attributed to the reduced degradation rate of
317 Erg11 at 37 °C compared to 30 °C. The slower degradation of Erg11 at 37 °C is due to
318 its degradation via autophagy, which is inhibited under this condition in *C. albicans*.
319 The inhibition of autophagy at 37 °C may be mediated by elevated mitochondrial
320 production of ROS, leading to mitochondrial dysfunction. In response to heat stress-
321 induced mitochondrial dysfunction, autophagy-related proteins such as Atg8
322 accumulate around the mitochondria, while their presence in the ER diminishes, thereby
323 suppressing autophagy in *C. albicans* (Figure 7).

324 Our investigation revealed that brief exposure of *C. albicans* to human body
325 temperature markedly increases the fungus's tolerance to azoles. This phenomenon may
326 significantly contribute to the ineffectiveness of azole treatments in infections caused
327 by non-resistant *C. albicans*. While the development of azole resistance in *C. albicans*
328 is a well-established cause of therapeutic failure, azole therapies may also prove
329 ineffective against infections involving non-resistant strains[4,38]. This ineffectiveness is
330 largely due to the intrinsic tolerance of *C. albicans* to azoles[4,12,38]. Previous studies have
331 confirmed that both in vitro and in vivo antifungal efficacy of FLC is substantially
332 reduced against *C. albicans* strains exhibiting high azole tolerance[7]. Research has
333 further shown that this tolerance is a pivotal factor in the persistence of candidemia[8,9].
334 Importantly, among patients who received their initial dose of FLC within 24 h of
335 candidemia onset, the probability of treatment failure was significantly higher when the
336 infecting strain demonstrated elevated tolerance to FLC[9]. This study illustrates that
337 even brief exposure to body temperature conditions can markedly increase the azole
338 tolerance of non-resistant *C. albicans*, potentially resulting in the ineffectiveness of
339 azole therapy for candidemia. These findings suggest that in the development of azole

340 adjuvants to augment antifungal efficacy against *C. albicans*, research should prioritize
341 evaluating whether these compounds facilitate the fungicidal action of azoles against
342 *C. albicans*[4,39,40].
343 Erg11 is integral to the biosynthesis of ergosterol and serves as a primary target for
344 azoles[41,42]. While the implications of Erg11 mutations and overexpression have been
345 extensively explored, its stability is equally crucial for maintaining fungal susceptibility
346 to azoles[43-45]. Current evidence suggests that Erg11 is processed via the Asi-mediated
347 Endoplasmic Reticulum-Associated Degradation (ERAD) pathway, which involves
348 ubiquitin-conjugating enzymes Ubc4 and Ubc7, the Asi1/Asi2/Asi3 ubiquitin ligase
349 complexes, and Cdc48-facilitated extraction, which culminates in Erg11 ubiquitination
350 and subsequent degradation in *S. cerevisiae*[30-32]. However, it remains uncertain whether
351 ubiquitinated Erg11 is degraded by the 26S proteasome—a pathway commonly
352 associated with many ERAD substrates[46]—or through autophagy, which is typical for
353 membrane proteins[47]. In this study, we demonstrated that the degradation of Erg11 is
354 inhibited by the autophagy inhibitor wortmannin, whereas the 26S proteasome inhibitor
355 MG132 did not significantly affect Erg11 degradation. Additionally, we observed that
356 Erg11 can translocate to the vacuole, suggesting that Erg11 in *C. albicans* is degraded
357 via autophagy. Our investigation further revealed that brief exposure to a body
358 temperature environment decelerates the degradation rate of Erg11 in *C. albicans* by
359 inhibiting the autophagy process, thereby affecting azole drug tolerance. This finding
360 expands the cognitive framework of azole tolerance mechanisms in *C. albicans*,
361 highlighting that host temperature can dynamically regulate the abundance of the target
362 enzyme Erg11 through epigenetic regulatory pathways.
363 In conclusion, this study demonstrates that under physiological temperature conditions,
364 the autophagy process in *C. albicans* is inhibited, leading to a reduced degradation rate
365 of Erg11. This inhibition consequently enhances the tolerance of *C. albicans* to azoles.
366 These findings suggest that promoting the degradation of Erg11 in *C. albicans* may
367 serve as a viable strategy to augment the fungicidal efficacy of azoles in the human
368 host.
369 **Methods**

370 **Plasmids, strains, primers, agents, and cultural conditions**

371 All plasmids, strains, and primers utilized in this study are detailed in Supplementary
372 Tables 1, 2, and 3, respectively. The *C. albicans* strains were cultured in YPD medium,
373 comprising 1% (w/v) yeast extract (Oxoid Ltd, Basingstoke, UK), 2% (w/v) peptone
374 (Oxoid Ltd, Basingstoke, UK), and 2% (w/v) glucose (Sangon Biotech, Shanghai,
375 China), at temperatures of either 30 °C or 37 °C. For the spotting assay, YPD medium
376 plates were supplemented with 2% (w/v) agar (Sangon Biotech, Shanghai, China) and
377 various concentrations of compounds. To construct mutant *C. albicans* strains, SD
378 selective medium was employed, consisting of 0.67% (w/v) yeast nitrogen base without
379 amino acids (Sangon Biotech, Shanghai, China), 2% (w/v) glucose, 2% (w/v) agar, and
380 an appropriate amino acid mix (Sangon Biotech, Shanghai, China). FLC, itraconazole,
381 miconazole, ketoconazole, voriconazole, fluvastatin, terbinafine, caspofungin, and
382 amphotericin B were procured from Aladdin, Shanghai, China. Myriocin, staurosporine,
383 brefeldin A, and amorolfine were obtained from MedChemExpress, Shanghai, China.
384 Tunicamycin was sourced from TargetMol, Boston, USA. All these compounds were
385 dissolved in dimethyl sulfoxide (DMSO) supplied by Sangon Biotech, Shanghai, China,
386 and stored at -20 °C.

387 **Spotting assays**

388 The spotting assay was performed as described previously[7]. FLC was dissolved in
389 DMSO, added to YPD medium, and used to prepare solid plates. Cultures of *C. albicans*
390 grown overnight were standardized to a concentration of 1×10^7 cells/ml in YPD. These
391 cultures were subsequently subjected to a series of 1:10 serial dilutions in YPD to five
392 concentration gradients. The plates were incubated at either 30 °C or 37 °C for a
393 duration of 48 h. Post-incubation, images of the plates were captured using the Tanon
394 5200 Imaging System (Tanon, Shanghai, China) in conjunction with AllDoc_X
395 software.

396 **In vitro antifungal susceptibility testing**

397 To examine the in vitro susceptibility to five azoles (FLC, itraconazole, miconazole,
398 ketoconazole, and voriconazole), other ergosterol biosynthesis inhibitors (terbinafine

399 and fluvastatin) and non-ergosterol biosynthesis antifungals (amphotericin B,
400 caspofungin, tunicamycin, myriocin, and staurosporine), the broth microdilution assay
401 was conducted according to previously reported protocol with slight modifications[48].
402 Briefly, 100 μl of drugs at 2-fold the final concentration was serially diluted in flat-
403 bottom 96-well plates and combined with 100 μl of overnight *C. albicans* cultures
404 adjusted to 1×10^3 cells/ml. The plates were incubated separately at 30 °C and 37 °C
405 without shaking, and the optical density at 600 nm (OD_{600}) was measured with a
406 spectrophotometer, Multiskan SkyHigh (Thermo Scientific, Singapore) after 24 h. The
407 MIC value was determined as the drug concentration at which 50% of the growth was
408 inhibited in terms of OD_{600} values compared to the no-drug wells.
409 To compare the values of SMG of FLC against different *Candida* isolates (*C. albicans*,
410 *C. parapsilosis*, *C. glabrata*, *C. krusei*, and *C. guilliermondii*), the *C. albicans* wild-
411 type strain SN152 and different mutants (*cdr1*Δ/Δ, *efg1*Δ/Δ, *ndt80*Δ/Δ, *upc2*Δ/Δ,
412 *erg24*Δ/Δ, and *erg251*Δ/Δ) between 30 °C and 37 °C, based on the broth microdilution
413 assay, the SMG value at 30 °C was calculated as the average growth per well above the
414 MIC divided by the level of growth without the drug, and the SMG at 37 °C was
415 calculated using the same MIC at 30 °C. The specific formula for calculating the value
416 of the SMG is as follows:

417 $$\mathrm{SMG} = \frac{\text{Average 24 h growth above MIC}}{\text{Growth without FLC}}$$

418 To examine whether one drug (cyclosporin A, terbinafine, fluvastatin, amorolfine,
419 wortmannin, MG132, and NAC) combined with FLC can clear trailing in *C. albicans*
420 at 30 °C and 37 °C, the checkerboard assays were used as described previously[49]. 50 μl
421 of 4-fold the final drug concentration of drug A was dispensed in 2-fold serial dilution
422 steps across plate columns, and then, 50 μl of 4-fold the final drug concentration of drug
423 B was dispensed in 2-fold serial dilution steps down rows of the plate. 100 μl of
424 overnight *C. albicans* cultures adjusted to 1×10^3 cells/ml was dispensed in all drug-
425 containing wells plus one control well containing no drugs. Cell concentrations were
426 recorded as the absorbance at OD_{600} after incubation at 30 °C or 37 °C for 24 h.
427 **The homozygous null mutants constructions**

428 To construct homozygous null mutants (*ndt80*Δ/Δ and *efg1*Δ/Δ) in this study, *C.*
429 *albicans* wild-type strain SN152 was used to permit disruption of both alleles of a given
430 target gene with two auxotrophic markers; In this experiment, the first round of gene
431 disruption was carried out with one of the three selectable markers, usually *Candida*
432 *dubliniensis* (*C. dubliniensis*) *HIS1*, and the second round was carried out with one of
433 the two remaining markers, usually *C. dubliniensis ARG4*. After selection of
434 transformants on the SD medium without histidine (SD/-His) or without histidine and
435 arginine (SD/-His/-Arg), gene disruption candidates were screened by PCR for
436 expected 5' and 3' junctions as well as the size of the disrupted gene[50].

437 **The doxycycline-inducible Tet-off promoter of genes mutants constructions**

438 To construct the doxycycline-inducible Tet-off promoter of *ERG11* or *ENO1* mutants,
439 first the *ERG11* and *ENO1* gene on one allele were deleted separately like what we
440 described above to generate *ERG11*/*erg11*Δ and *ENO1*/*eno1*Δ. Then the Tet-off vectors,
441 pCPC44 contained an ADH1 promoter, an ACT1 terminator and a tetracycline
442 repressor (TetR) element between them. TetR element was codon-optimized by
443 chemical synthesis and fused to GAL4AD to generate the fusion gene, *cat*TA. A
444 tetracycline-responsive elements (P_{Tet}) which was introduced into the downstream of
445 selection markers (*C. dubliniensis ARG4*). Through two rounds of PCR amplification
446 of pCPC44, the DNA cassettes with 78 bp homology regions to the target gene ($P_{tet\text{-}off}$-
447 *ERG11* and $P_{tet\text{-}off}$-*ENO1*) could be transformed into *ERG11*/*erg11*Δ and *ENO1*/*eno1*Δ
448 separately to generate the strain with the Tet-off promoter-controlled target gene. After
449 selection of transformants on the SD medium without arginine (SD/-Arg), verification
450 primers were used to verify the successful construction of the strain with the Tet-off
451 promoter-controlled *ERG11* or *ENO1* ($P_{tet\text{-}off}$-*ERG11*/*erg11*Δ and $P_{tet\text{-}off}$-
452 *ENO1*/*eno1*Δ)[51].

453 **The ectopic overexpression gene mutants constructions**

454 To construct the ectopic overexpression gene mutants, the ectopic overexpression
455 vectors, plasmids pCPC18-*ERG2*, pCPC18-*ERG4*, pCPC18-*ERG6*, pCPC18-*ERG9*,
456 pCPC18-*ERG11*, pCPC18-*ERG24*, pCPC18-*ERG26* and pCPC18-*ERG27* were
457 generated. In the plasmid pCPC18, the ADH1 promoter and the ACT1 terminator were

458 sequentially inserted into the coding region of the ADE2 gene and loxP-flanked
459 selection marker, *C. maltosa LEU2*, was placed downstream of the ACT1 terminator.
460 *ERG2*, *ERG4*, *ERG6*, *ERG9*, *ERG11*, *ERG24*, *ERG26* and *ERG27* open reading frame
461 (ORF) fragments were PCR amplified from *C. albicans* SN152 genomic DNA and
462 inserted into the plasmid pCPC18 backbone in one-step assembly reaction via Exo III-
463 mediated ligation-independent cloning (LIC)[51].
464 The plasmids, pCPC18-*ERG2*, pCPC18-*ERG4*, pCPC18-*ERG6*, pCPC18-*ERG9*,
465 pCPC18-*ERG11*, pCPC18-*ERG24*, pCPC18-*ERG26*, and pCPC18-*ERG27*, which we
466 described above were used to construct the ectopic overexpression mutants of *ERG2*,
467 *ERG4*, *ERG6*, *ERG9*, *ERG11*, *ERG24*, *ERG26* and *ERG27* in *upc2*Δ/Δ null mutant.
468 Through two rounds of PCR amplification, the ectopic expression cassettes were
469 transformed and integrated into the *ADE2* locus and were controlled by the constitutive
470 *ADH1* promoter. After selection of transformants on the SD medium without leucine
471 (SD/-Leu), verification primers were used to verify the successful construction of the
472 strain with the ectopic overexpression gene[51].
473 **RNA isolation and qRT–PCR**
474 The overnight cultured $P_{tet\text{-}off}$-*ERG11*/*erg11*Δ mutant and $P_{tet\text{-}off}$-*ENO1*/*eno1*Δ mutant
475 with the doxycycline (DOX)-inducible Tet-off promoter of *ERG11* or *ENO1* were
476 1:100 diluted to fresh YPD medium with different concentrations of DOX (0 μg/ml, 8
477 μg/ml, 16 μg/ml and 32 μg/ml; Aladdin, Shanghai, China) and cultured at 30 °C and
478 37 °C for 4 h to10^7 cells/ml and collected by centrifugation. RNA was isolated using
479 the YeaStar RNA Kit (Zymo reserch, USA). The quality of RNA preparations was
480 assessed by NanoDrop One (Thermo scientific, shanghai, China). One microgram of
481 RNA was used for complementary DNA (cDNA) synthesis using 5 × PrimeScript RT
482 Master Mix (Perfect Real Time) (Takara, Beijing, China). Quantitative reverse
483 transcriptasePCR (qRT–PCR) reactions were prepared using TB Green® Premix Ex
484 Taq™ II (Tli RNaseH Plus) (Takara, Beijing, China). cDNA mixtures were diluted 1:20
485 and 2 μl were used in a reaction volume of 20 μl with the primer pairs in Supplementary
486 Table 3 with the following cycle conditions: preincubation step was 95 °C for 30s; the
487 amplification step was 95 °C for 5s and 50 °C for 20s, repeat for 40 cycles in Bio-Rad

488 CFX Connect Real-Time System RT-PCR 96-well (Bio-Rad, Singapore). The levels of
489 gene expression with three replicates were determined in four separate amplifications
490 and analyzed using the 2^-ΔΔCt method. Relative levels of *ERG11* and *ENO1*
491 messenger RNA were normalized with respect to the levels of the invariant reference
492 gene *PGK1*; the levels of *ERG11* and *ENO1* in mutants treated with different
493 concentrations of DOX were subsequently averaged and normalized to the levels of
494 expression in the corresponding mutants without DOX.

495 **RNA-seq and data analysis**

496 *C. albicans* SN152 were overnight cultured at 30 °C and then 1:100 diluted to fresh
497 YPD medium cultured at 30 °C and 37 °C and collected at 4-hour, 8-hour and 16-hour
498 time points. Samples in biological triplicates were submitted to the BGISEQ platform
499 (BGI Genomics, Wuhan, China) for RNA sequencing analyzes. Transcriptome libraries
500 were generated using the Standard Sensitivity RNA Analysis Kit (15 nt) (DNF-471)
501 following the manufacturer's protocols performed by Fragment Analyzer. The raw
502 RNA-seq reads were quality controlled with SOAPnuke (v1.5.6)[52]. The trimmed reads
503 were mapped to the final assembly genomes *C. albicans* SC5314 (reference
504 candidagenome: Assembly22) using HISAT2 (v2.1.0)[53]. Bowtie2 (v2.3.4.3)[54] was used
505 to compare clean reads to reference gene sequences, and then RSEM (v1.3.1)[55] was
506 used to calculate gene expression levels for individual samples. DESeq2 (v1.4.5)[56] was
507 used to perform differential gene testing under the condition of Q value ≤ 0.05 or FDR
508 ≤ 0.001. GO enrichment analysis further explored the gene functions associated with
509 phenotypic changes. Based on hypergeometric testing, we used Phyper to perform GO
510 on differentially expressed genes enrichment analysis. The gene with Qvalue ≤ 0.05
511 was defined as significant enrichment in candidate genes that meet this condition. The
512 value of log2 Fold change (37 °C vs 30 °C) was not directly calculated by taking the
513 mean expression level (FPKM) and then calculating the log. Instead, it was
514 standardized using the local standard deviation of the FPKM (counts) based on a linear
515 regression of all gene expression levels, taking a small interval of the corresponding
516 gene, and then calculating the corresponding standard deviation. When correcting for

517 each mRNA expression level, it was related to the distribution of all mRNA expression
518 levels in each sample.

519 **Protein extractions and western blotting.**

520 To contrast the expression of Erg proteins (Erg6, Erg9, Erg10, Erg11, Erg12, Erg13,
521 Erg20, Erg26, and Erg251) between 30 °C and 37 °C, the *C. albicans* tagged ERG fused
522 to a C-terminal GFP were cultured overnight in YPD at 30 °C or 37 °C with shaking.
523 In order to examine the expression of Erg11 in the presence of FLC, the Erg11-GFP
524 mutants were cultured overnight in YPD at 30 °C and 1:10 diluted to fresh YPD
525 medium with or without 4 μg/ml FLC cultured at 30 °C or 37 °C for 4 h. All strains
526 were harvested at 4 °C, resuspended in 500 μl of protein lysis buffer which consists of
527 phosphate-buffered saline (PBS; Sangon biotech, Shanghai, China), 5 mM EDTA (pH
528 8.0; Sangon biotech, Shanghai, China), 1mM PMSF (Sangon biotech, Shanghai, China),
529 and 1.0% Protease Inhibitor cocktail (TargetMol, Shanghai, China), transferred into
530 screw-cap tubes with the addition of 500 μl of glass beads, and homogenized by a bead-
531 beater for 4 cycles of 1min, with 1 min cooling on ice in each cycle. Then the tubes
532 were centrifuged at 10,000 × g for 10 min at 4 °C and supernatant was transferred to a
533 new tube. The protein concentration was measured with Bradford Protein Assay Kit
534 (Epizyme, Shanghai, China). Equal amounts of protein were separated by 8-20% SDS-
535 PAGE (Byotime, Shanghai, China) and then transferred onto PVDF membranes (Merck
536 Millipore Ltd., Carrigtwohill, Ireland). After blocking with 1 × Protein Free Rapid
537 Blocking Buffer (Epizyme, Shanghai, China) for 10 min at room temperature, the
538 membranes were incubated with primary antibodies against GFP (Anti-GFP [B-2])
539 mouse monoclonal antibody, 1:1000 dilution; SANTA CRUZ BIOTECHNOLOGY,
540 USA) or α Tubulin (Anti-α Tubulin [YL1/2] rat monoclonal antibody, 1:1000 dilution;
541 SANTA CRUZ BIOTECHNOLOGY, USA) or Pgk1 (Anti-Pgk1 [14] mouse
542 monoclonal antibody, 1:1000 dilution; SANTA CRUZ BIOTECHNOLOGY, USA)
543 overnight at 4 °C. Then, the membranes were incubated with secondary antibodies
544 (Peroxidase-conjugated Anti-Mouse IgG_k, 1:10000 dilution; SANTA CRUZ

545 BIOTECHNOLOGY, USA) for 1 h at room temperature. The probed protein was
546 visualized using an ECL western blotting kit (Epizyme, Shanghai, China) and
547 photographed by the Tanon 5200 Chemiluminescence Imaging System (Tanon,
548 Shanghai, China) with AllDoc_X software. The α Tubulin and Pgk1 were used as the
549 loading control.

550 **Laser scanning confocal microscopy**

551 For the colocalization of Upc2 and nucleus, the Upc2-GFP mutants cultured overnight
552 at 30 °C were 1:10 diluted to YPD medium containing 16 μg/ml FLC and cultured at
553 30 °C or 37 °C for 4 h. After washing twice with PBS, cells were collected and
554 incubated with 10 μg/ml the nuclear dye, Hoechst 33342 (MedChemExpress, Shanghai,
555 China) for 10 min at room temperature in the dark. Finally, cells were washed with PBS
556 twice and photographed. The fluorescence distribution curve of the GFP green
557 fluorescence and nuclear dye (Hoechst) with a red fluorescent pseudocolor in the region
558 of interest in single cell was used to show the colocalization of Upc2 and nucleus at
559 30 °C and 37 °C by Image J (1.54g).

560 For the colocalization of Erg11 and vacuole, the Erg11-GFP mutant grown overnight
561 were 1:10 diluted to YPD medium and cultured at 30 °C or 37 °C for 1 h. After washing
562 twice with PBS, cells were collected and incubated with 100 μM vacuole dye,
563 CellTracker Blue CMAC (MedChemExpress, Shanghai, China) for 30 min at 30 °C or
564 37 °C in the dark. After washing with PBS twice, the cells were photographed. The
565 colocalization rate was calculated by dividing the number of cells colocalized showing
566 yellow fluorescence signal by the total number of cells.

567 For comparing the autophagy activity between 30 °C and 37 °C, the GFP-Atg8 mutants
568 grown overnight were 1:10 diluted to YPD medium and cultured at 30 °C or 37 °C for
569 1 h. After washing twice with PBS the cells were photographed. The autophagy activity
570 is reflected as the ratio of the number of cells with GFP-ATG8 dots to the total number
571 of cells at 30 °C and 37 °C.

572 For the colocalization of Atg8 and mitochondria or ER, the GFP-Atg8 mutants grown
573 overnight were 1:10 diluted to YPD mediut m and cultured at 30 °C or 37 °C for 30
574 min. After washing twice with PBS, cells were collected and incubated with 0.3 μM

575 mitochondria dye, MitoTracker Deep Red FM (MedChemExpress, Shanghai, China) or
576 1 μM ER dye, ER-tracker Red (MedChemExpress, Shanghai, China) for 30 min at
577 30 °C or 37 °C in the dark. After washing with PBS twice, the cells were photographed.
578 The colocalization ratio was calculated by dividing the number of GFP-Atg8 dots
579 colocalized with mitochondria or ER by the total number of cells containing GFP-Atg8
580 dots.
581 All the images were acquired on an Andor Dragonfly Confocal Imaging System (Andor,
582 Oxford instrument, UK), ImarisViewer (10.1.0) equipped with a white light laser. A
583 100 × oil-immersion objective was employed. The excitation (Ex)/emission (Em)
584 wavelength for GFP was 488 nm/521 nm. The Ex/Em wavelength of Hoechst 33342
585 for nucleus was 405 nm/445 nm. The Ex/Em wavelength of CellTracker Blue CMAC
586 for vacuole was 405 nm/445 nm. The Ex/Em of MitoTracker Deep Red FM for
587 mitochondria was 637 nm/660 nm. The Ex/Em of ER-tracker Red for ER was 572
588 nm/582 nm - 750 nm.
589 **Quantitation of the content of sterols**
590 The content of sterols in *C. albicans* was determined by a method described previously
591 with slight modifications[57]. *C. albicans* SN152 were overnight cultured at 30 °C and
592 then 1:100 diluted to fresh YPD medium cultured at 30 °C or 37 °C and collected at 4-
593 hour, 8-hour and 16-hour time points. For the group with FLC, *C. albicans* SN152 were
594 overnight cultured at 30 °C and then 1:100 diluted to fresh YPD medium with 16 μg/ml
595 FLC, cultured at 30 °C and 37 °C for 16 h. Cells were collected and washed three times
596 with double-distilled water (ddH2O), and the weight of the wet cell pellet was adjusted
597 to approximately 0.5 g. Furthermore, the 15% (m/v) NaOH (Sangon biotech, Shanghai,
598 China) dissolved in 90% (v/v) ethanol (Sangon biotech, Shanghai, China) were added
599 to each pellet and mixed thoroughly. The suspension was incubated at 80 °C for 1 h in
600 a water bath. Sterols were extracted by adding 18 ml of petroleum ether (boiling range:
601 30 °C-60 °C; SCR, Shanghai, China) in total three times, and each time the mixture was
602 vortexed vigorously for 2 min and allowed to stand for 3 min. The petroleum ether layer
603 was transferred to the same clear glass tubes and washed twice with ddH2O. The
604 collected petroleum ether was volatilized at 65 °C for 20 min in the water bath. Finally,

605 the sterols were extracted by the addition of 600 μl of n-hexane (Sangon biotech,
606 Shanghai, China), and a 200-μl aliquot was injected for gas chromatography-mass
607 spectrometry (Finnigan Voyager, USA) with HP-50 columns (50% phenyl–50%
608 methylpolysiloxane, 30 m by 0.25 mm by 0.25 μm). Before injection, 20 mg of
609 cholesterol (Sangon biotech, Shanghai, China) was added to each sample as the internal
610 reference for quantifying other sterols. Sterols of interest were identified by their
611 relative retention times, and mass spectra were compared with the sterol profiles of
612 NIST. The contents of sterol were calculated as the sterol mass corresponding to the
613 unit mass of cells (μg/mg). Assays were performed in duplicate three times.

614 **Cycloheximide chase analysis**

615 Cycloheximide (CHX) chase analysis was essentially performed by a method with
616 some modifications[58]. Briefly, The Erg11-GFP mutants were inoculated overnight in
617 YPD at 30 °C with shaking. The overnighted cultures were diluted to an OD_{600} value
618 of 0.2 in fresh YPD medium and incubated at 30 °C with shaking for about 4 h, until
619 the cells reach mid-logarithmic growth phase (OD_{600}=1.0). Then 25 OD_{600} units of each
620 culture per time point were collected. Then each cell pellet was resuspended in 10 ml
621 of 30 °C or 37 °C pre-warmed fresh YPD medium per 25 OD_{600} units of cells. After the
622 equilibrium of cell suspensions by incubation for 5 min in the 30 °C or 37 °C heat block,
623 cycloheximide (MedChemExpress, Shanghai, China) was added to a final
624 concentration of 1 mg/ml to the cell suspension and the timer started counting from
625 0:00. Immediately after adding cycloheximide and vertexing, 10 ml (~25 OD_{600} units)
626 of the cell suspension with added cycloheximide was transferred to a pre-cooling
627 microcentrifuge tube to centrifuge at 4,000 × g at 4 °C for 5 min. After that, the cell
628 suspension was removed the supernatant and washed with sterile water twice at 4,000
629 × g at 4 °C for 5 min and stored at -20 °C. When all samples at different time points
630 have been collected, the cells are ready to lysis for western blotting like we described
631 above. To investigate the effects of Wortmannin and MG132 on the degradation of
632 Erg11, Wortmannin (1 μM) and MG132 (100 μM) were added after adding
633 cycloheximide to inhibit the protein synthesis. Pgk1 was used as the loading control.
634 Assays were performed in duplicate three times.

635 **GFP–ATG8 cleavage assay**

636 In principle, GFP-Atg8 translocates along autophagosomes and is subsequently
637 released into vacuoles. GFP is more resistant to vacuolar hydrolases, leading to the
638 degradation of Atg8 while retaining GFP. Therefore, the ratio of free GFP to GFP–
639 ATG8 can reflect the activity of autophagy. To investigate the effect of different
640 temperatures on the activity of autophagy, the GFP-Atg8 mutants were overnight
641 cultured and then 1:10 diluted in YPD medium at 30 °C or 37 °C for 4 h. Total proteins
642 were extracted, measured with Bradford Protein Assay Kit and immunoblotted with
643 primary antibodies against GFP like what we describe in the western blotting assay.
644 Pgk1 was used as the loading control. The GFP cleavage activity was quantified by
645 determining the ratio of free GFP to GFP–ATG8.

646 **Measurement of intracellular reactive oxygen species**

647 Intracellular ROS was measured using 2',7'-dichlorodihydrofluoroscein diacetate
648 (DCFH-DA) with some modifications[59]. In principle, DCFH-DA entering the cell can
649 be hydrolyzed to form 2',7'-dichlorodihydrofluorescein (DCFH) which cannot permeate
650 cell membranes and then is oxidized by ROS to form fluorescent 2',7'-
651 Dichlorofluorescein (DCF). ROS level can be reflected by the measurement of
652 fluorescent DCF and calculation of specific fluorescence intensity (SFI). Specifically,
653 the *C. albicans* SN152 were overnight cultured at 30 °C and then 1:5 diluted and treated
654 with 10 μM DCFH-DA (MedChemExpress, Shanghai, China) and incubated at 30 °C
655 or 37 °C with shaking for 30 min. The cells were harvested at 4 °C and washed twice
656 with PBS. Then cells were suspended in 500 μl PBS and transferred into screw-cap
657 tubes with the addition of glass beads equal in volume to the cell pellet, and
658 homogenized by a bead-beater for 4 cycles of 1 min, with 1 min cooling on ice in each
659 cycle. Then the tubes were centrifuged at 10,000 × g for 10 min at 4 °C and supernatant
660 was transferred to a new tube. The fluorescence was recorded, at 25 °C, at an excitation
661 wavelength (Ex) of 485 nm and an emission (Em) wavelength of 535 nm, using the
662 microplate reader, Infinite F Plex (Tecan, Groedig, Austria). Em measurements were

663 normalized by estimation of the protein content of the supernatant using a Bradford
664 protein assay kit. The SFI was expressed as fluorescence [(Em = 535 nm/Ex = 485
665 nm)/mg protein]. As a control, background fluorescence of cells not treated with
666 DCFH-DA, was also recorded. In order to ensure that the fluorescence readings were
667 in the linear dynamic range of DCF concentrations (1 nM – 400 nM), a calibration curve
668 was constructed of fluorescence (Em = 535 nm, Ex = 485 nm) vs. DCF concentration.

669 **Growth curve assays**

670 Growth curve assay was performed as described previously[60]. *C. albicans* SN152 and
671 *atg8*Δ/Δ null mutant were overnight cultured at 30 °C. Then cells were adjusted to the
672 concentration of 10^3 cells/ml by the hemacytometer. Then cells were cultured at 30 °C
673 or 37 °C with shaking (200 rpm). The optical density at 600 nm (OD_{600}) was measured
674 every hour until the stationary phase of the growth curve was reached by using the
675 microplate reader, Infinite M Nano (Tecan, Groedig, Austria).

676 **Mitochondrial Membrane Potential (MMP)**

677 Changes in MMP were determined by the MMP probe JC-1 as previously described
678 with some modification. *C. albicans* SN152 and *atg8*Δ/Δ null mutant were overnight
679 cultured at 30 °C and then 1:10 diluted to fresh YPD medium cultured at 30 °C or 37 °C
680 for 4 h. Then cells were washed and resuspended in PBS with 2.5 μg/ml JC-1 at 37 °C
681 for 20 min in the dark, then washed twice. All samples were estimated via the BD
682 LSRFortessa Cell Analyzer (LSRFortessa; BD Bioscience, USA). Gating of single cells
683 was achieved as follows. The green fluorescence signal of the JC-1 monomer was
684 detected using the FITC channel equipped with a 530 nm band-pass filter (bandwidth
685 30 nm) while the red fluorescence signal of JC-1 aggregates was detected using the PE
686 channel equipped with a 585 nm band-pass filter (bandwidth 15 nm). First, the cells
687 populations were separated from cell debris and selected via SSC-A (side scatter; U =
688 302 V) and FSC-A (forward scatter; U = 640 V) signals. Second, duplet cells were
689 excluded via FSC-W and FSC-H signals. A total of 50,000 events was analyzed per
690 sample. Flow cytometry data were collected using FACS Diva Software and analysed
691 using FlowJo (10.8.1). SN152 cells cultured at 30 °C for 4 h with healthy mitochondria
692 were considered as negative control sample. Here, according to the negative control

693 sample, P1 was set as a region in which > 95% of the dual fluorescent population falls
694 within it and the JC-1 red/green fluorescence ratio > 1[61-63]. The loss of MMP was
695 reflected by the proportion of cells in P2 with less aggregates (red fluorescence) and
696 more monomer (green fluorescence) among different groups. The ordinary one-way
697 ANOVA, Bonferroni's multiple comparisons test was used to evaluate multiple
698 comparisons of the proportion of cells with damaged mitochondria.

699 **Statistical analysis**

700 Statistical analysis was performed using Graphpad Prism 9.0 software. The two-tailed
701 paired t-test was used to compare the values of SMG of FLC against clinical *Candida*
702 isolates (*C. glabrata*, *C. krusei* and *C. guilliermondii*) between 30 °C and 37 °C. The
703 Wilcoxon matched-pairs signed rank test was used to compare the values of SMG of
704 FLC against *C. albicans* and *C. parapsilosis* between 30 °C and 37 °C. The two-tailed
705 unpaired t-test was used to compare the expression of proteins in WB, sterol content,
706 the degradation of Erg11-GFP, the colocalization rate, the autophagic activity, Atg8
707 dots and ROS level between two groups. The ordinary one-way ANOVA, Bonferroni's
708 multiple comparisons test was used to evaluate multiple comparisons of the degradation
709 of Erg11-GFP in the presence of different compounds and the proportion of cells with
710 damaged mitochondria. For all analyses, $P < 0.05$ was considered significant. Data are
711 shown as means ± standard deviation (s.d.) from three or more replicates.

712 **Data availability**

713 The RNA sequencing data of *C. albicans* SN152 cultured at 30 °C and 37 °C for 4 h, 8
714 h and 16 h are publicly available at the NCBI Sequence Read Archive (SRA) and can
715 be accessed under BioProject PRJNA994182.

716 **Acknowledgments**

717 This study received financial support from the National Natural Science Foundation of
718 China (No. 82020108032), the Innovation Program of Shanghai Municipal Education
719 Commission (202101070007-E00094), and the National Key Research and
720 Development Program of China (No.2022YFC2303004).

721 **Author Contributions**

722 **YR.F.** conducted most of the experiments and performed data analysis. **YR.F.**, **H. L.,**
723 **M.W.,** and **YY.J.** wrote the manuscript draft and revised the manuscript. **YR.F., W.L.,**
724 **C.Z., XY.F,** and **XQ.S.** constructed mutant strains. **YR.F., W.L., C.Z., XY.F,** and
725 **XQ.S.** evaluated the antifungal activities and data collection. **YR.F., H. L., M. W.,** and
726 **YY.J.** discussed and analyzed the data. **H.L.** and **YY.J.** conceived the idea. **H.L.** and
727 **YY.J.** directed the experiments.

728 **Competing Interests statement**

729 The authors declare no conflicts of interest.

730

731 **References**

732 1 Lu, H., Hong, T., Jiang, Y., Whiteway, M. & Zhang, S. Candidiasis: From cutaneous to
733 systemic, new perspectives of potential targets and therapeutic strategies. *Adv Drug*
734 *Deliv Rev* **199**, 114960, doi:10.1016/j.addr.2023.114960 (2023).

735 2 Denning, D. W. Global incidence and mortality of severe fungal disease. *Lancet Infect*
736 *Dis* **24**, e428-e438, doi:10.1016/s1473-3099(23)00692-8 (2024).

737 3 Shafiei, M., Peyton, L., Hashemzadeh, M. & Foroumadi, A. History of the development
738 of antifungal azoles: A review on structures, SAR, and mechanism of action. *Bioorg*
739 *Chem* **104**, 104240, doi:10.1016/j.bioorg.2020.104240 (2020).

740 4 Berman, J. & Krysan, D. J. Drug resistance and tolerance in fungi. *Nat Rev Microbiol*
741 **18**, 319-331, doi:10.1038/s41579-019-0322-2 (2020).

742 5 Pfaller, M. A., Diekema, D. J., Turnidge, J. D., Castanheira, M. & Jones, R. N. Twenty
743 Years of the SENTRY Antifungal Surveillance Program: Results for Candida Species
744 From 1997-2016. *Open Forum Infect Dis* **6**, S79-S94, doi:10.1093/ofid/ofy358 (2019).

745 6 Lepak, A. J. & Andes, D. R. Antifungal pharmacokinetics and pharmacodynamics. *Cold*

746 *Spring Harb Perspect Med* **5**, a019653, doi:10.1101/cshperspect.a019653 (2014).

747 7 Li, W. *et al.* Pitavastatin Calcium Confers Fungicidal Properties to Fluconazole by
748 Inhibiting Ubiquinone Biosynthesis and Generating Reactive Oxygen Species.
749 *Antioxidants (Basel)* **13**, doi:10.3390/antiox13060667 (2024).

750 8 Rosenberg, A. *et al.* Antifungal tolerance is a subpopulation effect distinct from
751 resistance and is associated with persistent candidemia. *Nat Commun* **9**, 2470,
752 doi:10.1038/s41467-018-04926-x (2018).

753 9 Levinson, T. *et al.* Impact of tolerance to fluconazole on treatment response in Candida
754 albicans bloodstream infection. *Mycoses* **64**, 78-85, doi:10.1111/myc.13191 (2021).

755 10 Hammoud, M. S., Al-Taiar, A., Fouad, M., Raina, A. & Khan, Z. Persistent candidemia
756 in neonatal care units: risk factors and clinical significance. *Int J Infect Dis* **17**, e624-
757 628, doi:10.1016/j.ijid.2012.11.020 (2013).

758 11 Xu, Y. *et al.* Multifactorial Mechanisms of Tolerance to Ketoconazole in Candida
759 albicans. *Microbiol Spectr* **9**, e0032121, doi:10.1128/Spectrum.00321-21 (2021).

760 12 Yang, F. *et al.* Antifungal Tolerance and Resistance Emerge at Distinct Drug
761 Concentrations and Rely upon Different Aneuploid Chromosomes. *mBio* **14**, e0022723,
762 doi:10.1128/mbio.00227-23 (2023).

763 13 Huang, J. *et al.* Pan-drug resistance and hypervirulence in a human fungal pathogen
764 are enabled by mutagenesis induced by mammalian body temperature. *Nat Microbiol*
765 **9**, 1686-1699, doi:10.1038/s41564-024-01720-y (2024).

766 14 Fisher, M. C. *et al.* Tackling the emerging threat of antifungal resistance to human
767 health. *Nat Rev Microbiol* **20**, 557-571, doi:10.1038/s41579-022-00720-1 (2022).

768 15 Fisher, M. C., Hawkins, N. J., Sanglard, D. & Gurr, S. J. Worldwide emergence of
769 resistance to antifungal drugs challenges human health and food security. *Science* **360**,
770 739-742, doi:10.1126/science.aap7999 (2018).
771 16 Zhou, D. *et al.* Extensive Genetic Diversity and Widespread Azole Resistance in
772 Greenhouse Populations of Aspergillus fumigatus in Yunnan, China. *mSphere* **6**,
773 doi:10.1128/mSphere.00066-21 (2021).
774 17 Duong, T. N. *et al.* Azole-resistant Aspergillus fumigatus is highly prevalent in the
775 environment of Vietnam, with marked variability by land use type. *Environ Microbiol* **23**,
776 7632-7642, doi:10.1111/1462-2920.15660 (2021).
777 18 Daneshnia, F. *et al.* Worldwide emergence of fluconazole-resistant Candida
778 parapsilosis: current framework and future research roadmap. *Lancet Microbe* **4**, e470-
779 e480, doi:10.1016/S2666-5247(23)00067-8 (2023).
780 19 Casadevall, A., Kontoyiannis, D. P. & Robert, V. On the Emergence of Candida auris:
781 Climate Change, Azoles, Swamps, and Birds. *mBio* **10**, doi:10.1128/mBio.01397-19
782 (2019).
783 20 Akinbobola, A. B., Kean, R., Hanifi, S. M. A. & Quilliam, R. S. Environmental reservoirs
784 of the drug-resistant pathogenic yeast Candida auris. *PLoS Pathog* **19**, e1011268,
785 doi:10.1371/journal.ppat.1011268 (2023).
786 21 Bottery, M. J. & Denning, D. W. Body heat drives antifungal resistance. *Nat Microbiol*
787 **9**, 1638-1639, doi:10.1038/s41564-024-01738-2 (2024).
788 22 Lu, H. *et al.* A Small Molecule Inhibitor of Erg251 Makes Fluconazole Fungicidal by
789 Inhibiting the Synthesis of the 14alpha-Methylsterols. *mBio* **14**, e0263922,

790 doi:10.1128/mbio.02639-22 (2023).

791 23 Wang, H. *et al.* Myriocin enhances the antifungal activity of fluconazole by blocking the
792 membrane localization of the efflux pump Cdr1. *Front Pharmacol* **13**, 1101553,
793 doi:10.3389/fphar.2022.1101553 (2022).

794 24 Vasicek, E. M., Berkow, E. L., Flowers, S. A., Barker, K. S. & Rogers, P. D. UPC2 is
795 universally essential for azole antifungal resistance in Candida albicans. *Eukaryot Cell*
796 **13**, 933-946, doi:10.1128/ec.00221-13 (2014).

797 25 Lo, H. J. *et al.* Efg1 involved in drug resistance by regulating the expression of ERG3
798 in Candida albicans. *Antimicrob Agents Chemother* **49**, 1213-1215,
799 doi:10.1128/AAC.49.3.1213-1215.2005 (2005).

800 26 Sellam, A., Tebbji, F. & Nantel, A. Role of Ndt80p in sterol metabolism regulation and
801 azole resistance in Candida albicans. *Eukaryot Cell* **8**, 1174-1183,
802 doi:10.1128/EC.00074-09 (2009).

803 27 Yang, H. *et al.* Structural mechanism of ergosterol regulation by fungal sterol
804 transcription factor Upc2. *Nat Commun* **6**, 6129, doi:10.1038/ncomms7129 (2015).

805 28 Martel, C. M. *et al.* Identification and characterization of four azole-resistant erg3
806 mutants of Candida albicans. *Antimicrob Agents Chemother* **54**, 4527-4533,
807 doi:10.1128/AAC.00348-10 (2010).

808 29 Polak-Wyss, A., Lengsfeld, H. & Oesterhelt, G. Effect of oxiconazole and Ro 14-
809 4767/002 on sterol pattern in Candida albicans. *Sabouraudia* **23**, 433-441,
810 doi:10.1080/00362178585380631 (1985).

811 30 Foresti, O., Rodriguez-Vaello, V., Funaya, C. & Carvalho, P. Quality control of inner

812 nuclear membrane proteins by the Asi complex. *Science* **346**, 751-755,
813 doi:10.1126/science.1255638 (2014).
814 31 Natarajan, N., Foresti, O., Wendrich, K., Stein, A. & Carvalho, P. Quality Control of
815 Protein Complex Assembly by a Transmembrane Recognition Factor. *Mol Cell* **77**, 108-
816 119 e109, doi:10.1016/j.molcel.2019.10.003 (2020).
817 32 Khmelinskii, A. *et al.* Protein quality control at the inner nuclear membrane. *Nature* **516**,
818 410-413, doi:10.1038/nature14096 (2014).
819 33 Delorme-Axford, E., Guimaraes, R. S., Reggiori, F. & Klionsky, D. J. The yeast
820 Saccharomyces cerevisiae: an overview of methods to study autophagy progression.
821 *Methods* **75**, 3-12, doi:10.1016/j.ymeth.2014.12.008 (2015).
822 34 Marshall, R. S. & Vierstra, R. D. A trio of ubiquitin ligases sequentially drives
823 ubiquitylation and autophagic degradation of dysfunctional yeast proteasomes. *Cell*
824 *Rep* **38**, 110535, doi:10.1016/j.celrep.2022.110535 (2022).
825 35 Zhen, C. *et al.* Otilonium Bromide Exhibits Potent Antifungal Effects by Blocking
826 Ergosterol Plasma Membrane Localization and Triggering Cytotoxic Autophagy in
827 Candida Albicans. *Adv Sci (Weinh)*, e2406473, doi:10.1002/advs.202406473 (2024).
828 36 Chang-Chien, J. *et al.* Vitamin D ameliorates particulate matter induced mitochondrial
829 damages and calcium dyshomeostasis in BEAS-2B human bronchial epithelial cells.
830 *Respir Res* **25**, 321, doi:10.1186/s12931-024-02951-7 (2024).
831 37 Zhou, J. *et al.* A non-canonical role of ATG8 in Golgi recovery from heat stress in plants.
832 *Nat Plants* **9**, 749-765, doi:10.1038/s41477-023-01398-w (2023).
833 38 Feng, Y., Lu, H., Whiteway, M. & Jiang, Y. Understanding fluconazole tolerance in

834 Candida albicans: implications for effective treatment of candidiasis and combating
835 invasive fungal infections. *J Glob Antimicrob Resist* **35**, 314-321,
836 doi:10.1016/j.jgar.2023.10.019 (2023).
837 39 Xiong, J., Lu, H. & Jiang, Y. Mechanisms of Azole Potentiation: Insights from Drug
838 Repurposing Approaches. *ACS Infect Dis* **11**, 305-322,
839 doi:10.1021/acsinfecdis.4c00657 (2025).
840 40 Lu, H., Shrivastava, M., Whiteway, M. & Jiang, Y. Candida albicans targets that
841 potentially synergize with fluconazole. *Crit Rev Microbiol* **47**, 323-337,
842 doi:10.1080/1040841x.2021.1884641 (2021).
843 41 Jordá, T. & Puig, S. Regulation of Ergosterol Biosynthesis in Saccharomyces
844 cerevisiae. *Genes (Basel)* **11**, doi:10.3390/genes11070795 (2020).
845 42 Van Rhijn, N., Bromley, M., Richardson, M. & Bowyer, P. CYP51 Paralogue Structure
846 Is Associated with Intrinsic Azole Resistance in Fungi. *mBio* **12**, e0194521,
847 doi:10.1128/mBio.01945-21 (2021).
848 43 Hu, T. *et al.* Hotspot mutations and genomic expansion of ERG11 are major
849 mechanisms of azole resistance in environmental and human commensal isolates of
850 Candida tropicalis. *Int J Antimicrob Agents* **62**, 107010,
851 doi:10.1016/j.ijantimicag.2023.107010 (2023).
852 44 Handelman, M. *et al.* Point Mutation or Overexpression of Aspergillus fumigatus
853 cyp51B, Encoding Lanosterol 14alpha-Sterol Demethylase, Leads to Triazole
854 Resistance. *Antimicrob Agents Chemother* **65**, e0125221, doi:10.1128/AAC.01252-21
855 (2021).

856 45 Villasmil, M. L., Barbosa, A. D., Cunningham, J. L., Siniossoglou, S. & Nickels, J. T.,
857 Jr. An Erg11 lanosterol 14-alpha-demethylase-Arv1 complex is required for Candida
858 albicans virulence. *PLoS One* **15**, e0235746, doi:10.1371/journal.pone.0235746
859 (2020).
860 46 Krshnan, L., van de Weijer, M. L. & Carvalho, P. Endoplasmic Reticulum-Associated
861 Protein Degradation. *Cold Spring Harb Perspect Biol* **14**,
862 doi:10.1101/cshperspect.a041247 (2022).
863 47 Li, Y., Li, S. & Wu, H. Ubiquitination-Proteasome System (UPS) and Autophagy Two
864 Main Protein Degradation Machineries in Response to Cell Stress. *Cells* **11**,
865 doi:10.3390/cells11050851 (2022).
866 48 Lu, H. *et al.* A Small Molecule Inhibitor of Erg251 Makes Fluconazole Fungicidal by
867 Inhibiting the Synthesis of the 14α-Methylsterols. *mBio* **14**, e0263922,
868 doi:10.1128/mbio.02639-22 (2023).
869 49 Epp, E. *et al.* Reverse genetics in Candida albicans predicts ARF cycling is essential
870 for drug resistance and virulence. *PLoS Pathog* **6**, e1000753,
871 doi:10.1371/journal.ppat.1000753 (2010).
872 50 Noble, S. M. & Johnson, A. D. Strains and strategies for large-scale gene deletion
873 studies of the diploid human fungal pathogen Candida albicans. *Eukaryot Cell* **4**, 298-
874 309, doi:10.1128/ec.4.2.298-309.2005 (2005).
875 51 Chang, P., Wang, W., Igarashi, Y., Luo, F. & Chen, J. Efficient vector systems for
876 economical and rapid epitope-tagging and overexpression in Candida albicans. *J*
877 *Microbiol Methods* **149**, 14-19, doi:10.1016/j.mimet.2018.04.016 (2018).

878 52 Li, R., Li, Y., Kristiansen, K. & Wang, J. SOAP: short oligonucleotide alignment program.
879 *Bioinformatics* **24**, 713-714, doi:10.1093/bioinformatics/btn025 (2008).
880 53 Kim, D., Langmead, B. & Salzberg, S. L. HISAT: a fast spliced aligner with low memory
881 requirements. *Nat Methods* **12**, 357-360, doi:10.1038/nmeth.3317 (2015).
882 54 Langmead, B. & Salzberg, S. L. Fast gapped-read alignment with Bowtie 2. *Nat*
883 *Methods* **9**, 357-359, doi:10.1038/nmeth.1923 (2012).
884 55 Li, B. & Dewey, C. N. RSEM: accurate transcript quantification from RNA-Seq data with
885 or without a reference genome. *BMC Bioinformatics* **12**, 323, doi:10.1186/1471-2105-
886 12-323 (2011).
887 56 Love, M. I., Huber, W. & Anders, S. Moderated estimation of fold change and dispersion
888 for RNA-seq data with DESeq2. *Genome Biol* **15**, 550, doi:10.1186/s13059-014-0550-
889 8 (2014).
890 57 Lv, Q. Z. *et al.* NSG2 (ORF19.273) Encoding Protein Controls Sensitivity of Candida
891 albicans to Azoles through Regulating the Synthesis of C14-Methylated Sterols. *Front*
892 *Microbiol* **9**, 218, doi:10.3389/fmicb.2018.00218 (2018).
893 58 Buchanan, B. W., Lloyd, M. E., Engle, S. M. & Rubenstein, E. M. Cycloheximide Chase
894 Analysis of Protein Degradation in Saccharomyces cerevisiae. *J Vis Exp*,
895 doi:10.3791/53975 (2016).
896 59 Moraitis, C. & Curran, B. P. Reactive oxygen species may influence the heat shock
897 response and stress tolerance in the yeast Saccharomyces cerevisiae. *Yeast* **21**, 313-
898 323, doi:10.1002/yea.1078 (2004).
899 60 Lu, H. *et al.* Loss of RPS41 but not its paralog RPS42 results in altered growth,

filamentation and transcriptome changes in Candida albicans. *Fungal Genet Biol* **80**, 31-42, doi:10.1016/j.fgb.2015.03.012 (2015).

61 Guthrie, H. D. & Welch, G. R. Determination of intracellular reactive oxygen species and high mitochondrial membrane potential in Percoll-treated viable boar sperm using fluorescence-activated flow cytometry. *J Anim Sci* **84**, 2089-2100, doi:10.2527/jas.2005-766 (2006).

62 Yamakawa, K. *et al.* Platelet mitochondrial membrane potential correlates with severity in patients with systemic inflammatory response syndrome. *J Trauma Acute Care Surg* **74**, 411-417; discussion 418, doi:10.1097/TA.0b013e31827a34cf (2013).

63 Elefantova, K., Lakatos, B., Kubickova, J., Sulova, Z. & Breier, A. Detection of the Mitochondrial Membrane Potential by the Cationic Dye JC-1 in L1210 Cells with Massive Overexpression of the Plasma Membrane ABCB1 Drug Transporter. *Int J Mol Sci* **19**, doi:10.3390/ijms19071985 (2018).

915 **Figures**

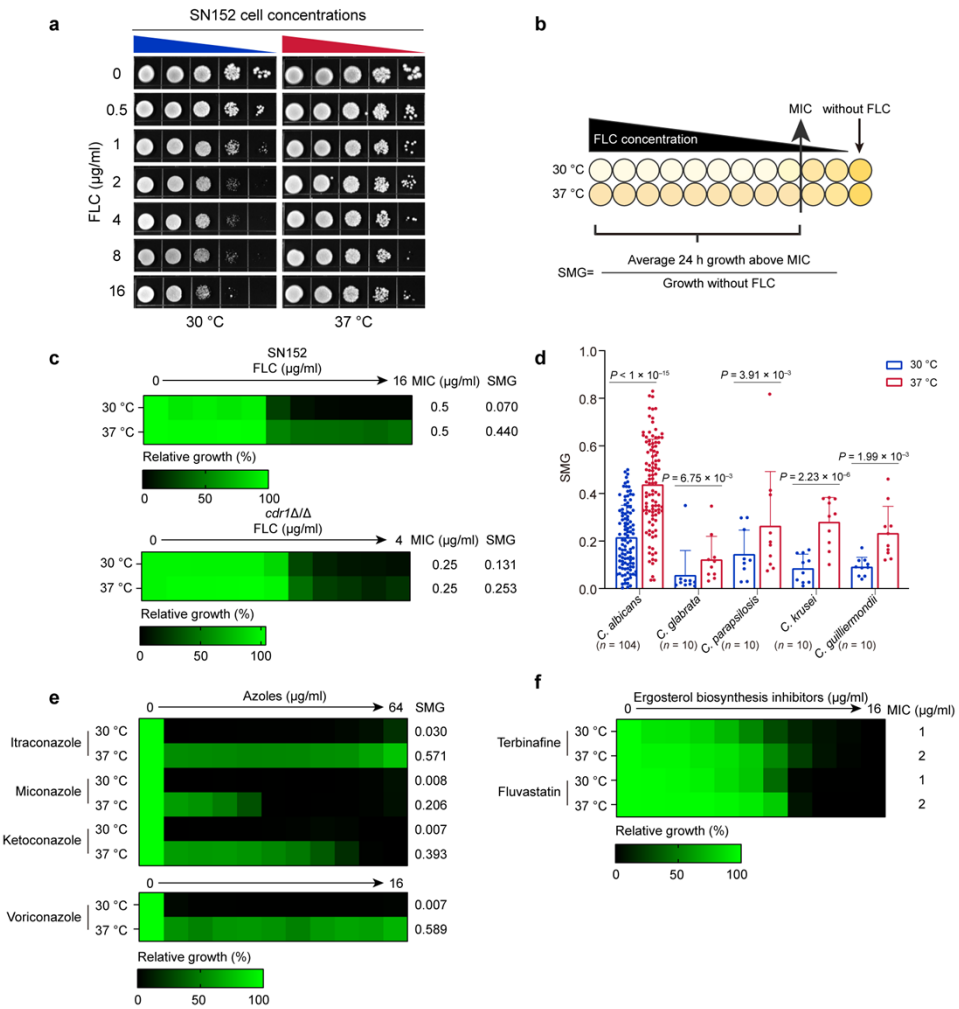

916

917 **Figure 1.** Short-term exposure to body temperature enhances the tolerance of *C.*
918 *albicans* to azoles. **(a)** Spotting assays of *C. albicans* SN152. Cells were spotted onto
919 YPD agar containing different concentrations (0 μg/ml, 0.5 μg/ml, 1 μg/ml, 2 μg/ml, 4
920 μg/ml, 8 μg/ml and 16 μg/ml) of fluconazole (FLC) and cultured at 30 °C or 37 °C for
921 2 days. The different colors of right triangle indicate cells were 1:10 serially diluted and
922 cultured at 30 °C (blue one) or 37 °C (red one). (**b**) Illustration of minimum inhibitory
923 concentration (MIC) and supra-MIC growth (SMG) calculations. MIC was calculated
924 at 24 h as the FLC concentration at which 50% of the growth was inhibited at 30 °C,
925 relative to growth without FLC. SMG was calculated as the average growth per well
926 above the MIC divided by the level of growth without FLC. The darker the yellow color,
927 the more vigorous the cell growth. **c**, Broth microdilution assays showing MIC and

928 SMG levels at 24 h for *C. albicans* wild-type SN152 and *cdr1*Δ/Δ null mutant cultured
929 at 30 °C or 37 °C in the presence of FLC. **d**, The values of SMG of FLC against clinical
930 *Candida* isolates which were cultured at 30 °C or 37 °C. Data represent mean ± standard
931 deviation (s.d). The *P* values were determined by the Wilcoxon matched-pairs signed
932 rank test for *C. albicans* ($n = 104$) and *C. parapsilosis* ($n = 10$) and the two-tailed paired
933 *t* test for *C. glabrata* ($n = 10$), *C. krusei* ($n = 10$) and *C. guilliermondii* ($n = 10$). **e**, Broth
934 microdilution assays showing SMG levels at 24 h for *C. albicans* SN152 cultured at
935 30 °C or 37 °C in the presence of azoles. Technical duplicates were averaged. **f**, Broth
936 microdilution assays showing MIC levels at 24 h for *C. albicans* SN152 cultured at
937 30 °C or 37 °C in the presence of terbinafine and fluvastatin. Technical duplicates were
938 averaged.
939

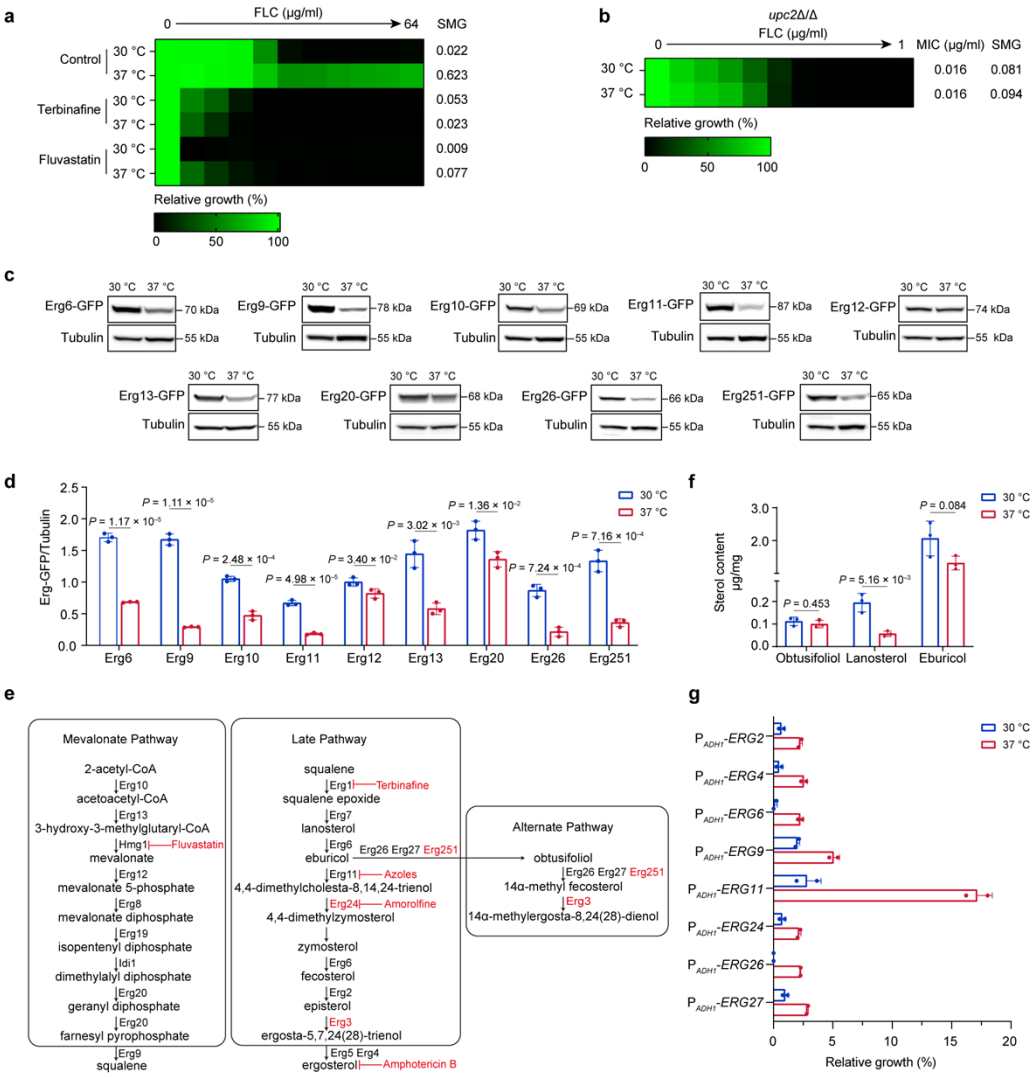

Figure 2. Body temperature enhances *C. albicans*' tolerance to azoles through Erg11. **a**, Broth microdilution assays showing SMG levels at 24 h for *C. albicans* SN152 cultured at 30 °C or 37 °C in the presence of FLC combined with fluvastatin (1 μg/ml) or terbinafine (1 μg/ml). The control group represents cells were in the presence of FLC without combined compounds. **b**, Broth microdilution assays showing MIC and SMG levels at 24 h for *upc2*Δ/Δ null mutant cultured at 30 °C or 37 °C in the presence of FLC. Technical duplicates were averaged. **c**, The expression of proteins involved in ergosterol synthesis (Erg6, Erg9, Erg10, Erg11, Erg12, Erg 13, Erg20, Erg26 and Erg251) examined by western blotting. Cells were precultured at 30 °C or 37 °C for 16 h. The representative images shown are from three replicates. **d**, Quantification of the signal intensity ratio of Erg-GFP to Tubulin by Image J. Data represent means ± s.d. of

952 three replicates, two-tailed, unpaired t test. **e**, Illustration of ergosterol synthesis
953 pathway and ergosterol synthesis inhibitors. **f**, The determination of sterol content in
954 the presence of 16 μg/ml FLC based on GC-MS at the 16-hour time point. Data
955 represent means ± s.d. of three replicates, two-tailed, unpaired t test. **g**, The relative
956 growth at optical density at 600 nm (OD_{600}) of *upc2*Δ/Δ null mutants in which the
957 expression of ergosterol biosynthesis genes (*ERG2*, *ERG4*, *ERG6, ERG9*, *ERG11*,
958 *ERG24, ERG26*, and *ERG27*) were increased by ADH1 promoter in the presence of
959 0.25 μg/ml FLC at 30 °C or 37 °C for 24 h. Technical duplicates were averaged.
960

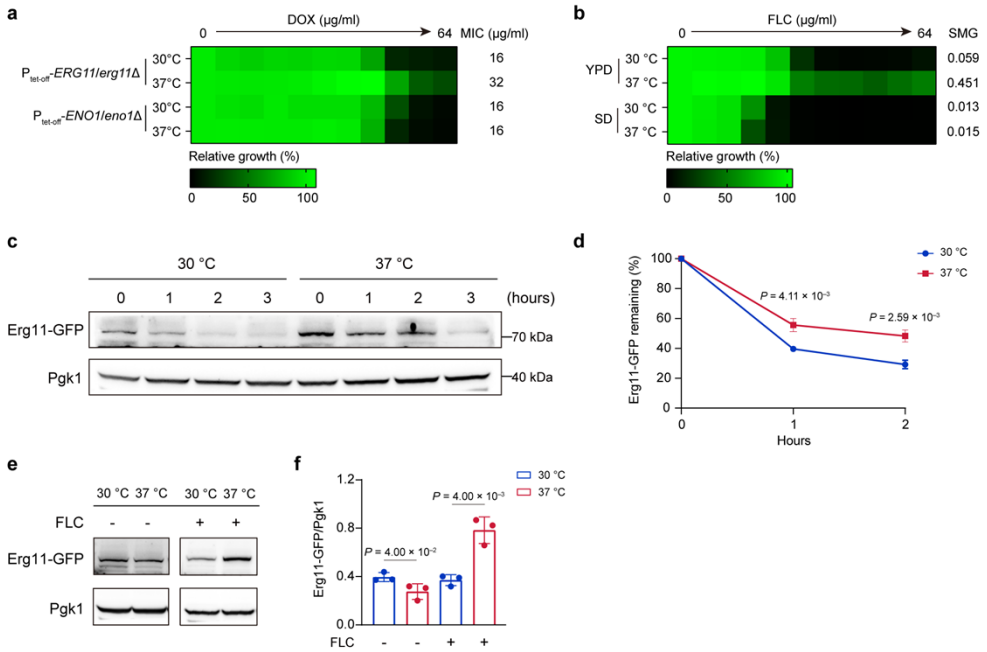

Figure 3. Body temperature inhibits the degradation of Erg11. **a**, Broth microdilution assays showing MIC levels at 24 h for $P_{tet\text{-}off}$-*ERG11*/*erg11*Δ mutant and $P_{tet\text{-}off}$-*ENO1*/*eno1*Δ mutant cultured at 30 °C or 37 °C in the presence of DOX. Technical duplicates were averaged. **b**, Broth microdilution assays showing SMG levels at 24 h for *C. albicans* SN152 cultured in different culture medium (YPD or SD) at 30 °C or 37 °C in the presence of FLC. Technical duplicates were averaged. **c**, Degradation of Erg11-GFP in *C. albicans* SN152 after inhibition of protein synthesis by cycloheximide upon a 3-hour shift to 30 °C or 37 °C. The representative images shown are from three replicates. **d**, Quantification of the degradation of Erg11-GFP calculated as the ratio of Erg11-GFP to Pgk1 by Image J. Set the protein level at the initial time point to 100 %. Data represent means ± s.d. of three replicates, two-tailed, unpaired t test. **e**, The expression of Erg11 protein examined by western blotting. Cells were precultured at 30 °C and 37 °C for 4 h with or without 4 μg/ml FLC. The representative images shown are from three replicates. **f**, Quantification of the signal intensity ratio of Erg11-GFP to Pgk1 by Image J. Data represent means ± s.d. of three replicates, two-tailed, unpaired t test.

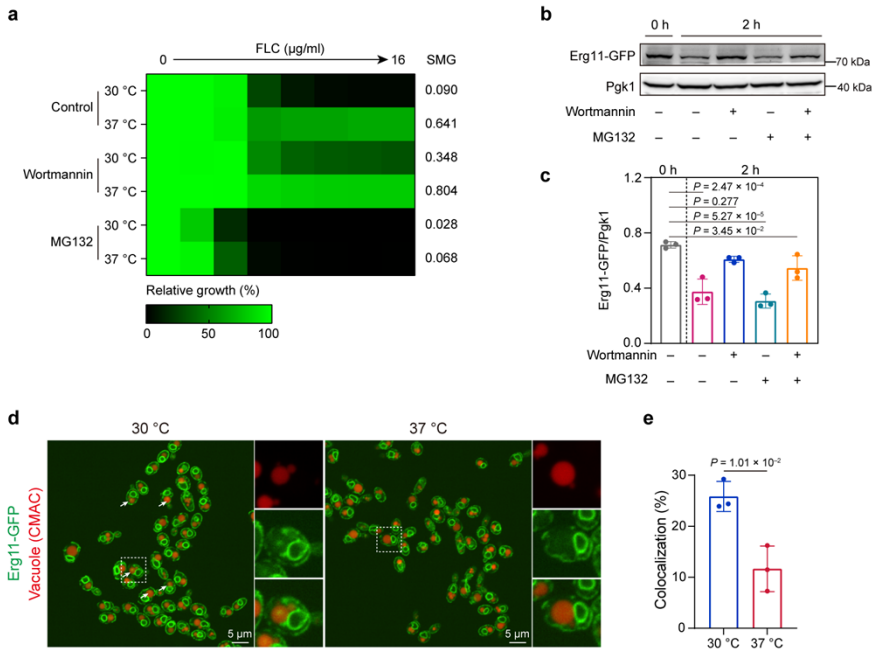

Figure 4. Erg11 undergoes degradation through autophagy. **a**, Broth microdilution assays showing SMG levels at 24 h for *C. albicans* SN152 cultured at 30 °C or 37 °C in the presence of FLC combined with wortmannin (1 μM) or MG132 (6.25 μM). Technical duplicates were averaged. **b**, Degradation of Erg11-GFP in *C. albicans* SN152 in the presence of Wortmannin (1 μM) and MG132 (100 μM) after inhibition of protein synthesis by cycloheximide upon a 2-hour shift to 30 °C. **c**, Quantification of the degradation of Erg11-GFP calculated as the ratio of Erg11-GFP to Pgk1 by Image J. Data represent means ± s.d. of three replicates, ordinary one-way ANOVA, Bonferroni's multiple comparisons test. **d**, Colocalization between Erg11-GFP and vacuole in cells precultured at 30 °C or 37 °C for 1 h. Pseudo-color was used to display the blue fluorescence of the vacuole dye (CellTracker Blue CMAC) as red. The white arrow indicated vacuoles with Erg11-GFP. The representative images shown are from three replicates. Scale bar, 5 μm. **e**, Quantification of the colocalization ratio of the number of cells colocalized with Erg11 and vacuoles to the total number of cells. The data represent means ± s.d of three replicates, two-tailed, unpaired t test.

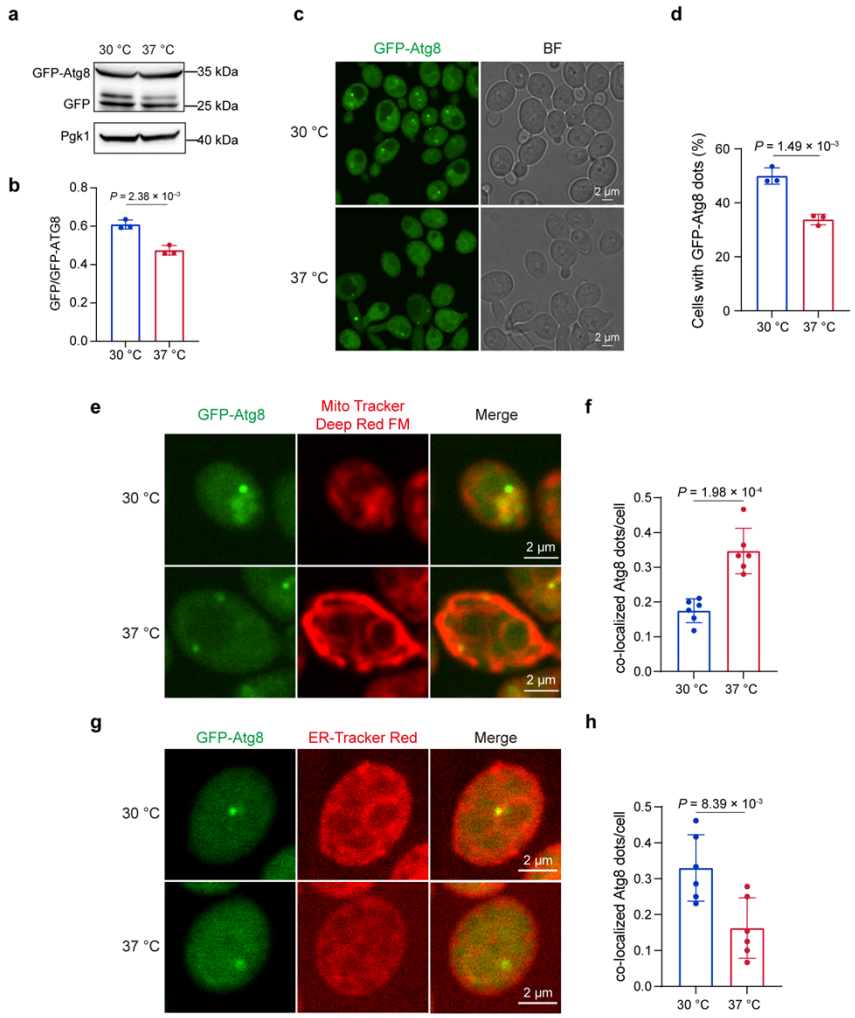

Figure 5. Body temperature inhibits autophagy in *C. albicans*. **a**, GFP-ATG8 cleavage assay showing the autophagic activity after pre-cultivation at 30 °C or 37 °C for 4 h. **b**, Quantification of the autophagic activity displaying as the ratio of free GFP to GFP-ATG8 by Image J. Data represent means ± s.d. of three replicates, two-tailed, unpaired t test. **c**, Confocal images of GFP-ATG8 dots in cells precultured at 30 °C or 37 °C for 1 h. BF represents cells in bright filed. Scale bar, 2 μm. **d**, The ratio of the number of cells with GFP-ATG8 dots to the total number of cells. Data represent means ± s.d. form three replicates, two-tailed, unpaired t test. **e**, Colocalization between GFP-Atg8 dots and mitochondria in cells precultured at 30 °C or 37 °C for 30 min. Scale bar, 2 μm. **f**, Quantification of the colocalization ratio of the number of GFP-Atg8 dots colocalized with mitochondria to the number of cells containing GFP-Atg8 dots. The data represent means ± s.d. n = 6 confocal microscopic images form three replicates, two-tailed,

1010 unpaired t test. **g**, Colocalization between GFP-Atg8 dots and ER in cells precultured
1011 at 30 °C or 37 °C for 30 min. Scale bar, 2 μm. **h**, Quantification of the colocalization
1012 ratio of the number of GFP-Atg8 dots colocalized with ER to the number of cells
1013 containing GFP-Atg8 dots. The data represent means ± s.d. n = 6 confocal microscopic
1014 images form three replicates, two-tailed, unpaired t test.
1015

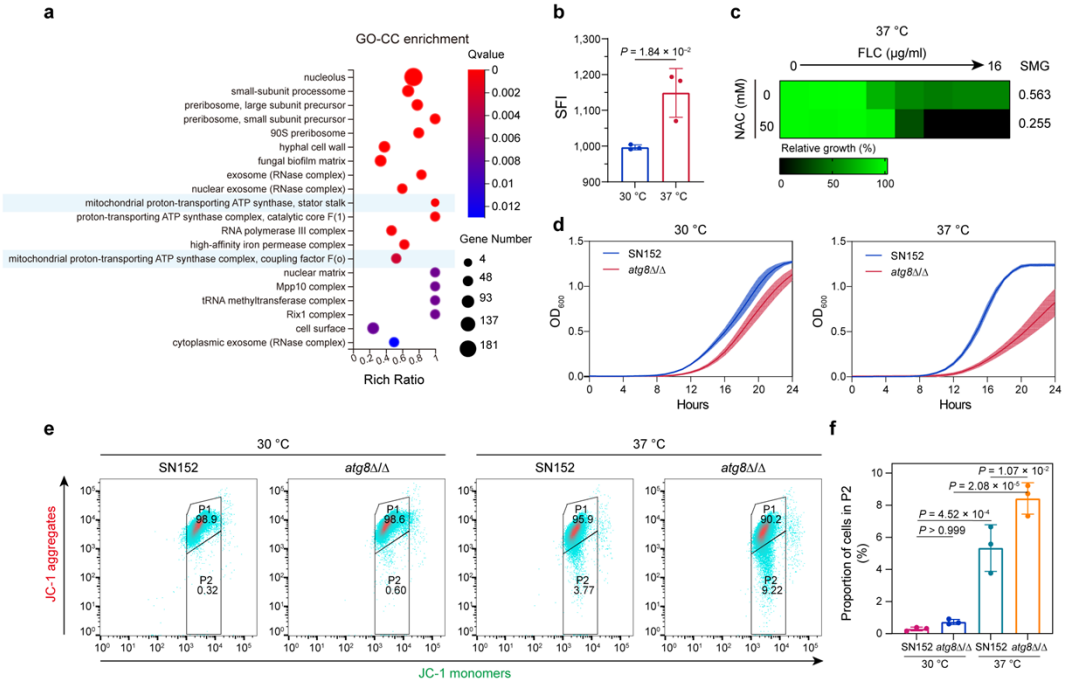

Figure 6. Atg8 relocalizes to mitochondria to safeguard them against oxidative damage induced by Body temperature. **a**, Gene Ontology categories according to cellular components (GO-CC) enrichment based on the 1733 genes with significant differences of expression level (Qvalue ≤ 0.05) in *C. albicans* SN152 cultured at 30 °C and 37 °C for 4 h. **b**, The intracellular ROS levels measured by specific fluorescence intensity (SFI) of the oxidant-sensitive probe 2′,7′-dichlorofluorescin diacetate (DCFH-DA) in cells precultured at 30 °C or 37 °C for 30 min. SFI was calculated as fluorescence [(Em = 535 nm/Ex = 485 nm)/mg protein]. Data represent means ± s.d. of three replicates, two-tailed, unpaired t test. **c**, Broth microdilution assays showing SMG levels at 24 h for *C. albicans* SN152 cultured at 37 °C in the presence of FLC combined with NAC (0 mM and 50mM). Technical duplicates were averaged. **d**, Growth curve of *C. albicans* SN125 (blue) and *atg8*Δ/Δ null mutant (red) at 30 °C (left) and 37 °C (right) for 24 h. The optical density at 600 nm (OD_{600}) was measured every hour. The colored bands show the means ± s.d. of six replicates. **e**, Determination of mitochondrial membrane potential (MMP) by JC-1 for *C. albicans* SN125 and the *atg8*Δ/Δ null mutant at 30 °C and 37 °C for 4 h through flow cytometry. JC-1 aggregates show red fluorescence (FL-1 channel, y-axis) and JC-1monomer shows green fluorescence (FL-

1034 2 channel, x-axis). Healthy cells were classified in P1, while cells with damaged
1035 mitochondria were classified in P2. The representative images shown are from three
1036 replicates. **f**, Quantification of the proportion of cells in P2 with damaged mitochondria
1037 by FlowJo. Data represent means ± s.d. of three replicates, ordinary one-way ANOVA,
1038 Bonferroni's multiple comparisons test.

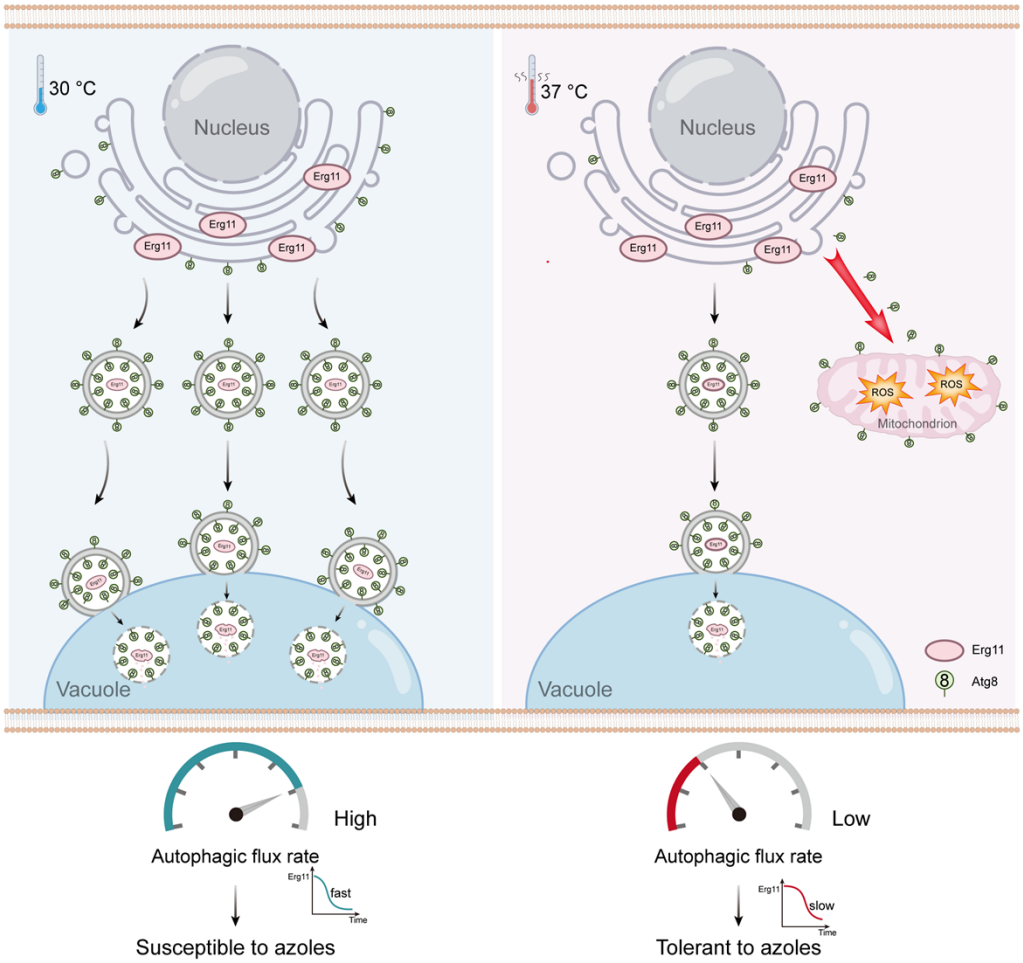

Fig.7 Schematic diagram showing a model of body temperature-induced azoles tolerance. Compared with 30 °C, body temperature (37 °C) results in an elevated mitochondrial production of ROS and subsequently leads to mitochondrial dysfunction which causes the relocation of Atg8 to mitochondria and the inhibition of autophagy. As the result, the slower degradation of Erg11 results in azole tolerance in *C. albicans* at 37 °C.